Geological Society of America Bulletin

Geologic correlation of the Himalayan orogen and Indian craton: Part 1. Structural geology, U-Pb zircon geochronology, and tectonic evolution of the Shillong Plateau and its neighboring regions in NE India

An Yin, C.S. Dubey, A.A.G. Webb, T.K. Kelty, M. Grove, G.E. Gehrels and W.P. Burgess

---

Notes

THE
GEOLOGICAL
SOCIETY
OF AMERICA

Geologic correlation of the Himalayan orogen and Indian craton: Part 1. Structural geology, U-Pb zircon geochronology, and tectonic evolution of the Shillong Plateau and its neighboring regions in NE India

An Yin[1,2,†], C.S. Dubey[3], A.A.G. Webb[1], T.K. Kelty[4], M. Grove[5], G.E. Gehrels[6], and W.P. Burgess[1]

[1]*Department of Earth and Space Sciences and Institute of Geophysics and Planetary Physics, University of California, Los Angeles, California 90095, USA*

[2]*Structural Geology Group, School of Earth Sciences and Resources, China University of Geosciences (Beijing), Beijing 10083, China*

[3]*Department of Geology, Delhi University, Delhi-110007, India*

[4]*Department of Geological Sciences, California State University at Long Beach, Long Beach, California 90840-3902, USA*

[5]*Department of Geological and Environmental Sciences, Stanford University, Stanford, California 94305, USA*

[6]*Department of Geosciences, University of Arizona, Tucson, Arizona 85721, USA*

ABSTRACT

The Himalayan orogen has experienced intense Cenozoic deformation and widespread metamorphism, making it difficult to track its initial architecture and the subsequent deformation path during the Cenozoic India-Asia collision. To address this issue, we conducted structural mapping and U-Pb zircon geochronology across the Shillong Plateau, Mikir Hills, and Brahmaputra River Valley of northeastern India, located 30–100 km south of the eastern Himalaya. Our work reveals three episodes of igneous activity at ca. 1600 Ma, ca. 1100 Ma, and ca. 500 Ma, and three ductile-deformation events at ca. 1100 Ma, 520–500 Ma, and during the Cretaceous. The first two events were contractional, possibly induced by assembly of Rodinia and Eastern Gondwana, while the last event was extensional, possibly related to breakup of Gondwana. Because of its proximity to the Himalaya, the occurrence of 500 Ma contractional deformation in northeastern India implies that any attempt to determine the magnitude of Cenozoic deformation across the Himalayan orogen using Proterozoic strata as marker beds must first remove the effect of early Paleozoic deformation. The lithostratigraphy of the Shillong Plateau established by this study and its correlation to the Himalayan units imply that the Greater Himalayan Crystalline Complex may be a tectonic mixture of Indian crystalline basement, its Proterozoic-Cambrian cover sequence, and an early Paleozoic arc. Although the Shillong Plateau may be regarded as a rigid block in the Cenozoic, our work demonstrates that distributed active left-slip faulting dominates its interior, consistent with earthquake focal mechanisms and global positioning system velocity fields across the region.

INTRODUCTION

Understanding the tectonic evolution of an orogen requires detailed knowledge of its original architecture, which serves as a strain marker and initial condition for determining the magnitude of deformation and tracking the deformation path responsible for its formation. The active Himalayan orogen has experienced intense Cenozoic deformation, high-grade metamorphism, and widespread syncollisional anatexis (e.g., LeFort, 1996; Yin, 2006). These processes have created many uncertainties in reconstructing the original geologic framework and thus the evolution of the Himalayan orogen. For example, the three main Himalayan tectono-stratigraphic units, the Greater Himalayan Crystalline Complex, the Lesser Himalayan Sequence (LHS), and the Tethyan Himalayan Sequence (THS), are all juxtaposed by orogen-scale faults (Gansser, 1964; LeFort, 1996; Yin and Harrison, 2000; DiPietro and Pogue, 2004), making it exceedingly challenging to establish their original stratigraphic relationships prior to the Cenozoic India-Asia collision (DeCelles et al., 2000; cf. Myrow et al., 2003; also see review by Yin, 2006). A central point to this issue is the tectonic origin of the Greater Himalayan Crystalline Complex, which makes up the core of

the Himalaya; it has been inferred to be derived from the Indian crystalline basement (Heim and Gansser, 1939; Gansser, 1964; LeFort, 1975), an exotic terrane (DeCelles et al., 2000), or Tibetan middle crust north of the Indus-Tsangpo suture (Nelson et al., 1996; cf. Beaumont et al., 2001, 2004, 2006). Each of these models makes distinctive predictions about the protolith of the Greater Himalayan Crystalline Complex and implies different kinematic histories and dynamic controls for Himalayan development. An Indian-basement origin for the Greater Himalayan Crystalline Complex requires the orogen to have formed by thick-skinned thrusting (e.g., Gansser, 1964; LeFort, 1975; Yin et al., 2006). An exotic-terrane hypothesis predicts the Himalayan orogen to have been built by reactivation of a major early Paleozoic suture (DeCelles et al., 2000; Gehrels et al., 2003, 2006a, 2006b; cf. Frank et al., 1995; Miller et al., 2000; Steck, 2003; Myrow et al., 2003). Finally, derivation of the Greater Himalayan Crystalline Complex from Tibetan middle crust north of the Indus-Tsangpo suture argues for large-scale horizontal middle-crustal flow during continental collision (Nelson et al., 1996).

One way to address the origin of the Greater Himalayan Crystalline Complex is to establish the pre-Cenozoic structural and stratigraphic frameworks of the Himalayan orogen and its neighboring Tibetan Plateau and Indian craton (Fig. 1). This paper represents the first of two papers on this issue by focusing on the geology of the Shillong Plateau, Mikir Hills, and Brahmaputra River Valley in the northeastern Indian craton (Fig. 1). The companion paper will deal with the geology of the eastern Himalaya,

---

†E-mail: yin@ess.ucla.edu.
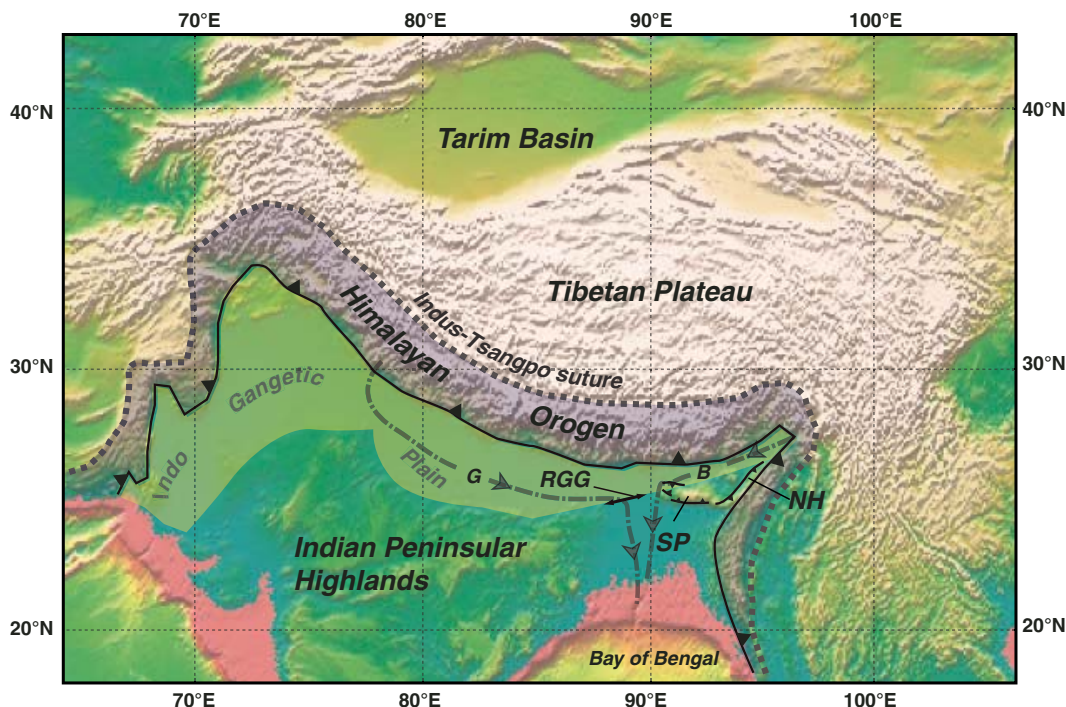
Figure 1. Outline of the Himalayan orogen between the Indus-Tsangpo suture zone and the northern edge of the Indo-Gangetic plain and the locations of the Shillong Plateau (SP), Rajmahal-Garo Gap (RGG), and Naga Hills (NH). The Ganges River (G) and Brahmaputra River (B) both flow across the Rajmahal-Garo Gap into the Bay of Bengal.

respectively (Yin et al., 2009). We select northeastern India for this study because its basement rocks are located as close as only ~30 km from the Himalayan front (Fig. 2A) (Gansser, 1983; Das Gupta and Biswas, 2000), which provides more confidence for geologic correlations. Below, we describe the regional geology of the Shillong Plateau and its surrounding regions and report the results of our structural mapping, U-Pb geochronologic analysis, and regional tectonic reconstruction. Our work not only provides new constraints on the original geologic framework of the Himalayan orogen but also has broader implications for the evolution of Eastern Gondwana during the terminal Proterozoic.

REGIONAL GEOLOGY

The Shillong Plateau is a northward-tilting topographic feature, and its highest peaks reach ~2 km along its southern rim. The plateau is separated from the Indian Peninsular Highlands by the north-trending Rajmahal-Garo Gap at which the Brahmaputra and Ganges Rivers meet (Fig. 1). The plateau is bounded in the south by the north-dipping Dauki fault and its related folds (Evans, 1964; Biswas and Grasemann, 2005), in the east by the northwest-striking, right-slip Kapili fault and the Naga Hills thrust belt (Evans, 1964; Kayal et al., 2006), in the north by the Oldham and Brahmaputra Valley faults (Bilham and England, 2001; Gupta

and Sen, 1988; Rajendran et al., 2004), and in the west by the Jamuna fault (Gupta and Sen, 1988; Nakata, 1989) (Fig. 2A). Internally, the Shillong Plateau exhibits a series of northeast-trending and locally north-trending linear topographic features, which have been interpreted as extensional fissures related to Cretaceous Gondwana breakup (Gupta and Sen, 1988; Kumar et al., 1996; Srivastava and Sinha, 2004a, 2004b; Srivastava et al., 2005). The late Cenozoic uplift of the Shillong Plateau may have exerted a strong influence on the spatially varying exhumation history and stress distribution across the eastern Himalaya (Bilham and England, 2001; Grujic et al., 2006).

At ~35 km, the crustal thickness of the Shillong Plateau is slightly thinner than its surrounding regions (Mitra et al., 2005). The Moho north of the Shillong Plateau dips gently northward and reaches a depth of ~44 km at the Himalayan front (Kumar et al., 2004; Ramesh et al., 2005; Mitra et al., 2005) (Fig. 2B). Strike-slip focal mechanisms dominate the Shillong Plateau; the seismicity occurs across all depths of the crust and may even be in the uppermost mantle (Kayal and De, 1991; Mitra et al., 2005; Drukpa et al., 2006). Shear wave anisotropy in northeastern India exhibits an east-west fastest direction below the Himalaya, a north-south fastest direction across the Indian-Burma Range, and a northeast-southwest fastest direction across the Shillong Plateau (Singh et al., 2006), all of which correlate well with surface

traces of Cenozoic faults (also see Kumar et al., 1996).

The basement of the Shillong Plateau consists of sillimanite-bearing paragneiss, amphibolites, banded iron formations, granulites, and orthogneiss (e.g., Ghosh et al., 2005). The orthogneiss units yield Rb-Sr whole-rock isochron ages of ca. 1700 Ma, ca. 1400 Ma, ca. 1100 Ma, ca. 800 Ma, ca. 700 Ma, and 600–420 Ma (Crawford, 1969; van Breemen et al., 1989; Ghosh et al., 1991, 1994, 2005). The widely scattered Rb-Sr ages can be attributed to several factors. First, the analytical errors are quite large, ranging from 15 m.y. to 122 m.y. (e.g., van Breemen et al., 1989; Ghosh et al., 1991). Second, the Rb-Sr ages may represent cooling rather than crystallization ages. Third, the method cannot detect multiple thermal events and thus may have produced error chron ages with no geologic significance. Because of these complexities, the crystallization ages of plutons in the Shillong Plateau are poorly constrained, and this has made the correlation of Himalayan and Indian units difficult. It also limits our ability to decipher the tectonic events across Eastern Gondwana (e.g., Collins and Pisarevsky, 2005). The timing of metamorphism in the Shillong crystalline basement has been determined by the chemical ages of metamorphic monazites, with ages clustered at 1600–1400 Ma, 1000–1300 Ma, and ca. 500 Ma, respectively (Chatterjee et al., 2007). These metamorphic age clusters are in

Yin et al.
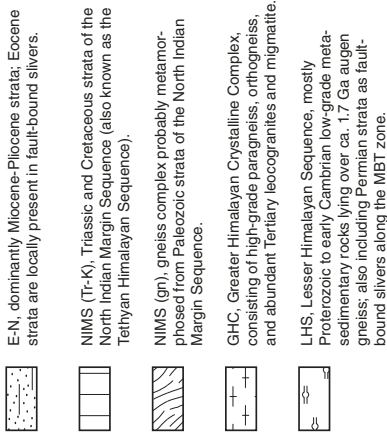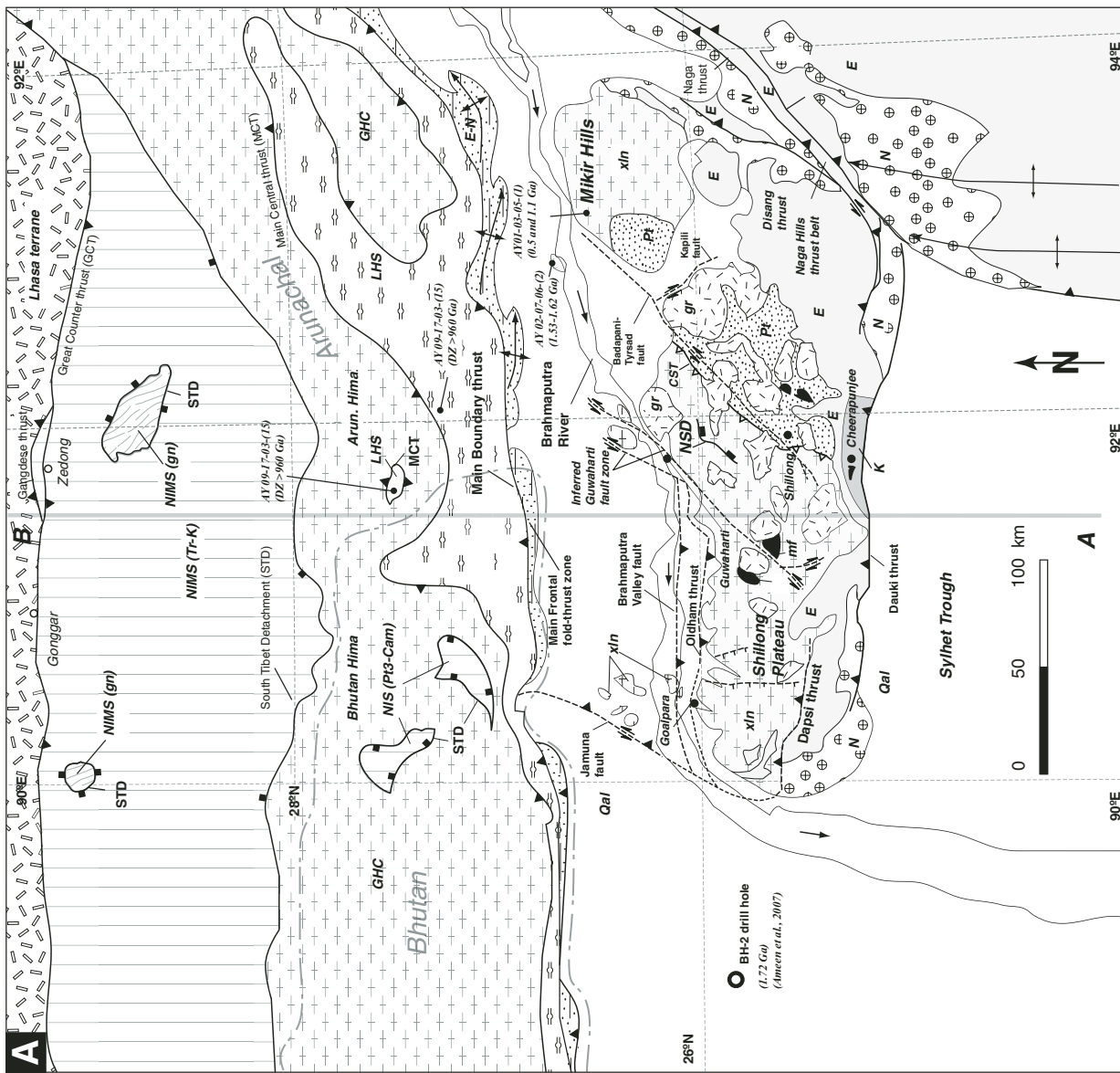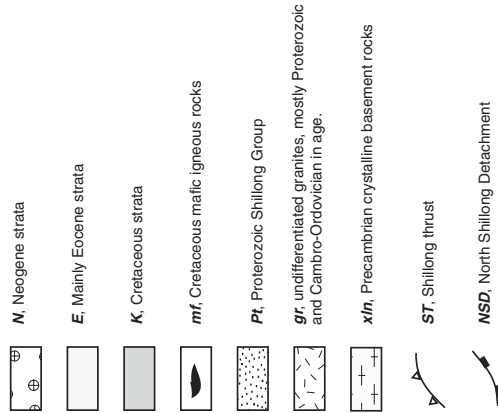
Figure 2. (A) Tectonic map of the eastern Himalaya and the Shillong Plateau, compiled from Pan et al. (2004), Srivastava and Sinha (2004a, 2004b), Ghosh et al. (2005), and our own field observations. Lithologic units in the eastern Himalaya are as follows: NIMS (gn)—gneiss in the North India Margin Sequence (also known as the Tethyan Himalayan Sequence), NIMS (Tr-K)—Triassic and Cretaceous metasedimentary strata in the North Indian Margin Sequence; GHC—Greater Himalayan Crystalline Complex; LHS—Lesser Himalayan Sequence; N—Neogene strata, locally associated with Paleogene and Permian strata in the Main Boundary thrust (MBT) fault zone. Lithologic units in the Shillong Plateau and its adjacent regions are defined as follows: xln—crystalline basement rocks; Pt—Proterozoic Shillong Group overlying the crystalline basement; gr—undifferentiated granites; K—Cretaceous strata; E—Paleogene strata; N—Neogene strata; Q—Quaternary strata. (*Continued on following page.*)

338   Geological Society of America Bulletin, March/April 2010
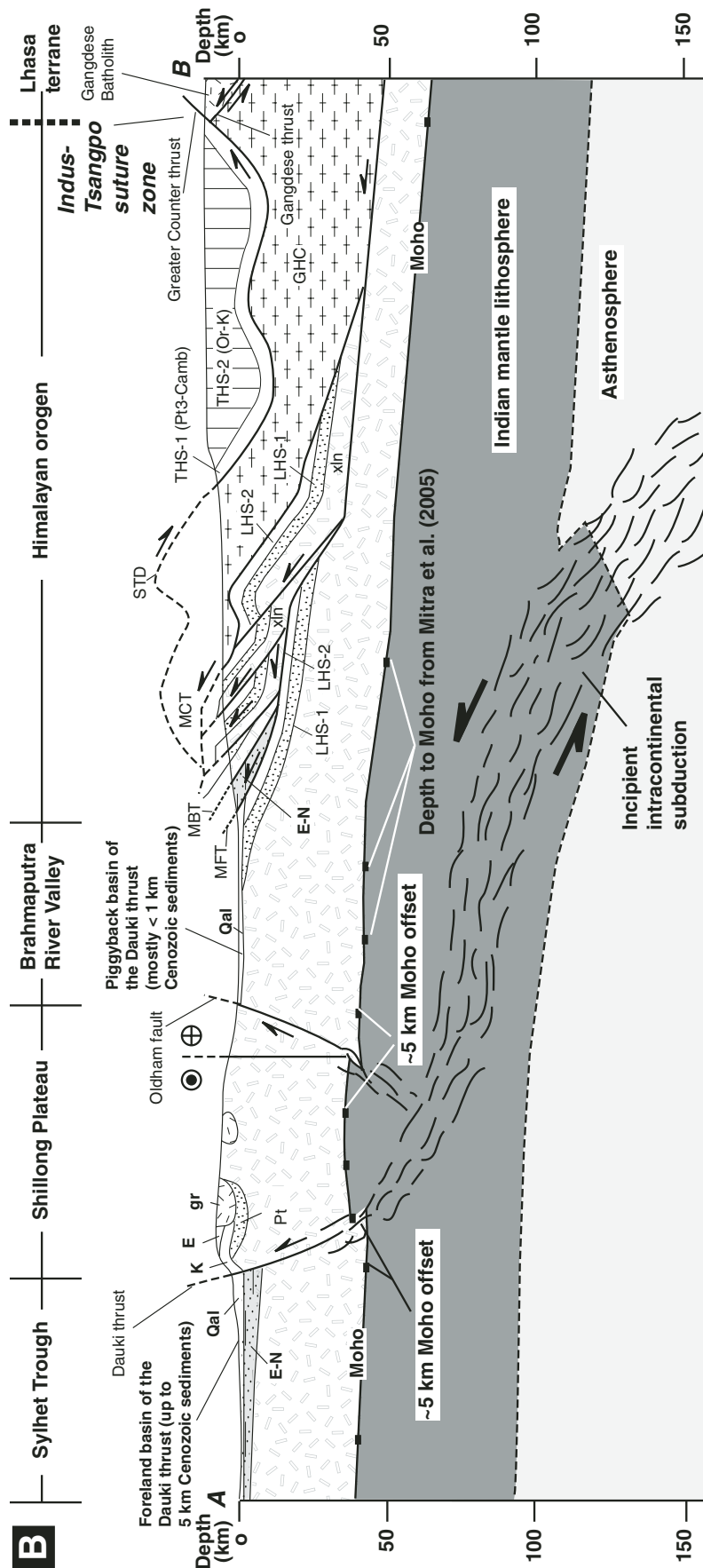
Shillong Plateau

Figure 2 *(continued)*. **(B)** Schematic cross section across the Shillong Plateau and the eastern Himalaya. Lithologic correlation between Himalayan units and those in the Shillong plateau is also indicated based on the results of this study. LHS1 is the lower Lesser Himalayan Sequence that has a Mesoproterozoic age; LHS2 is the upper Lesser Himalayan Sequence that has a Late Proterozoic and Early Cambrian age (e.g., Hughes et al., 2005); THS1 is the lower Tethyan Himalayan Sequence that has a late Proterozoic to Cambrian age possibly correlative with the LHS2; THS1 is the Greater Himalayan Crystalline Complex possibly correlative with the combined crystalline basement of Indian craton (xln), Proterozoic and Cambrian-Ordovician granitoids (gr), and Mesoproterozoic to Cambrian sedimentary cover sequence of the Indian craton (Pt2/3 + Cam). The depth to Moho follows Mitra et al. (2005).

strong contrast to the nearly continuous Rb-Sr ages in the region. As shown here, our U-Pb zircon geochronology supports the notion that the Shillong region experienced episodic rather than semicontinuous thermal events in the same time periods broadly delineated by Chatterjee et al. (2007).

The cover sequence of the Shillong Plateau consists of the Proterozoic Shillong Group, Permian Gondwana sequence, and Cretaceous to Neogene sediments (Das Gupta and Biswas 2000) (Fig. 2A). The Shillong Group consists of quartz arenite, sandstone, and phyllite, all of which have experienced multiple phases of folding and, locally, lower greenschist-facies metamorphism (Ghosh et al., 1994; Mitra and Mitra, 2001). Deposition of the Cretaceous sediments (mostly sandstone and shale) was associated with 150–105 Ma basaltic ultrama-fic-alkaline-carbonatite extrusions (e.g., Lal et al., 1978; Srivastava and Sinha, 2004a, 2004b; Srivastava et al., 2005). The occurrence of the Cretaceous mafic and ultramafic rocks has been related to Gondwana breakup and coeval formation of the Kerguelen oceanic plateau at 110–120 Ma (Coffin et al., 2002; Srivastava et al., 2005).

Although continuous Cenozoic stratigraphic sections exist in the Naga Hills in the east and the Bengal Basin (also known as Sylhet Trough) in the south, Oligocene strata are missing and Miocene strata are much thinner over much of the Shillong Plateau than those in the Bengal Basin in the south (Evans, 1964; Das Gupta and Biswas, 2000). This relationship may be explained by progressive growth and uplift of the Shillong Plateau since the early Miocene (ca. 23 Ma), which is much earlier than the inferred Pliocene initiation of the Shillong uplift at ca. 5 Ma (Johnson and Alam, 1991). Apatite (U-Th)/He and fission-track thermochronology indicates protracted cooling between 114 Ma and 8 Ma across the central plateau, where the older ages are possibly related to Gondwana breakup and the younger ages (14–8 Ma) are related to Cenozoic uplift of the Shillong Plateau (Clark, 2006; Biswas et al., 2006, 2007).

GEOLOGY OF THE CENTRAL SHILLONG PLATEAU AND NEIGHBORING REGIONS

We conducted mapping along the main road from Guwahati to Cheerapunjee across the central Shillong Plateau (Fig. 2). We also examined crystalline rocks in the Brahmaputra River Valley and northern Mikir Hills, where we collected critical samples to date the main ortho-gneiss units and the age of ductile deformation. We describe our main findings next.

Shillong Plateau

Lithology

A major lithologic unit encountered in our traverse is an undifferentiated crystalline complex (unit xln in Fig. 3A) that is composed of quartzo-feldspathic gneiss, garnet schist, ortho-gneiss, and locally amphibolite. This unit is intruded by large deformed granitoids having a longest dimension >10 km (unit gr-1 in Fig. 3A). The gr-1 unit itself is intruded by deformed and undeformed granitoids and their associated dikes and veins (unit gr-2 in Fig. 3A). Unit gr-1 is mostly biotite granitoid and locally contains lenses of mafic xenoliths ~30–50 cm long and 10–20 cm wide. Unit gr-2 is mostly K-feldspar granitoid. As shown by our U-Pb zircon dating, gr-1 has an age of ca. 1100 Ma, while gr-2 has an age of 520–480 Ma.

The Shillong Group along our traverse is made up of phyllite, mudstone, sandstone, and coarse-grained cross-bedded quartz arenite. Due to isoclinal folding (Fig. 4D) and the lack of continuous exposure, we could not establish the general stratigraphy of the Shillong Group. The contact between the crystalline basement and the Shillong Group is not exposed, although it can be determined within ~20 m in the field. The crystalline basement next to the buried contact is highly altered schist, whereas beds of the Shillong Group next to the contact are phyllite that is isoclinally folded with axial cleavage completely transposing its original bedding. The intensity of the deformation and cleavage development decrease rapidly away from the contact in the Shillong Group, and the original sedimentary structures such as cross-bedding are visible in sandstones ~1–2 km away from the contact. The decrease in the intensity of deformation is also evident from our mapping; directly against the contact, there is a tight syncline in the Shillong Group and the fold limbs dip at 69° and 75°, respectively (Fig. 3A). The dip of the beds decreases rapidly to become ~24° ~4–5 km away from the contact (Fig. 3A). Finally, the bedding becomes steep again as it approaches the left-slip Badapani-Tyrsad fault. These observations suggest that the basement–Shillong Group contact is most likely tectonic (see detailed discussion later herein) (Fig. 3A).

Eocene strata overlie the Shillong Group and include coal-bearing sandstone, mudstone, and shale (Fig. 4B). They are either flat-lying or very broadly folded (Fig. 3A). South of the Eocene exposure, there are Cretaceous strata, consisting of thickly bedded basalt, siltstone, mudstone, and sandstone. The Cretaceous beds are nearly flat-lying in the north (Fig. 4F) but become steep (~65°) in the south as they approach the Dauki fault zone (Fig. 3A). This relationship suggests

that the Cretaceous strata were probably nearly horizontal prior to Cenozoic deformation, and their steep dips in the south were induced by Cenozoic deformation.

Ductile Structures

Ductile deformation in the central Shillong Plateau is expressed by the formation of gneissic foliation in the crystalline basement, axial cleavage in both the crystalline basement and the Shillong Group strata, tight to isoclinal folds in the Shillong Group, and ductile shear zones in the crystalline basement. Although the strike of the gneissic foliation in the Shillong Plateau and its neighboring regions is dominantly northeast, the dip directions vary across a series of antiforms and synforms in the basement, with a wavelength of 5–8 km (Fig. 3A). Axial cleavage is commonly associated with the basement folds, which trend northeast parallel to the northeast-trending folds in the Shillong Group and the contact between the basement and the Shillong Group. The parallel relationship among the regional gneissic foliation, folds, and major lithologic contacts implies that these structures were formed penecontemporaneously under the same compressional event.

Our mapping revealed a major ductile shear zone in the northern Shillong Plateau. It places a garnet-bearing metapelite unit (mpl in Fig. 3A) over a metamorphic unit composed of quartzo-feldspathic gneiss (unit gn in Fig. 3A). The shear zone is at least 20 m thick, striking N15°E and dipping 55°SE. Stretching mineral lineation in the shear zone trends N65°E and plunges 40°. Asymmetric porphyroblasts indicate an oblique-normal sense of shear with the east side of the shear zone down. Fold hinges in the shear zone are parallel to the stretching lineation, which may have resulted from large simple-shear deformation causing the fold axes to rotate ~90°. The metapelite unit is intruded by leucogranitic dikes of unknown age that are isoclinally folded. Despite folding of gneissic foliations in its hanging wall and footwall, the ductile shear zone itself is not folded, suggesting that its development postdates regional contraction. This observation has important implications for constraining its possible age of motion. We refer to the ductile shear zone as the North Shillong Detachment (Fig. 3). We note at several places that this shear zone is cut by brittle faults striking N20°E. Although we could not determine the kinematics of the brittle faults in the field, their parallelism to the nearby active left-slip faults suggests that they might be Cenozoic in age (Fig. 3A).

Major Brittle Faults

Major faults encountered by our mapping include (1) the northeast-striking Badapani-

Tyrsad fault system, (2) the northeast-striking Central Shillong thrust (see following discussion), and (3) the Dauki thrust zone. We observed the Badapani-Tyrsad fault system at two locations. The first is at the northern end of the fault zone in the northeastern corner of our study area (Fig. 3A), where the fault enters the Brahmaputra River Valley (location 1 in Fig. 3A). A minor fault in the fault zone that cuts an orthogneiss unit strikes N60ºE and dips 80ºSE. Striations on this fault trend N60ºE and plunge 25º (Fig. 3A). This fault consistently offsets veins and gneissic foliations in a left-lateral shear sense. The second place we examined the Badapani-Tyrsad fault zone is near the town of Mawiyngkhung, ~10 km north of the city of Shillong (location 2 in Fig. 3A and Fig. 5A). There, the shear zone is composed of steeply dipping phyllite of the Shillong Group. The shear zone strikes N45ºE and dips 86ºSE (Figs. 5A and 5B). It also exhibits subhorizontal stretching lineation. The angular relationship between the shear zone and the cleavage within the shear zone indicates a left-slip sense of shear.

The Badapani-Tyrsad fault system has a prominent topographic expression, and its trace follows a series of north-northeast–trending linear valleys and ridges in the interior Shillong Plateau (Fig. 5). For this reason, we suspect that the fault is active. We tested this speculation by examining satellite images downloaded from Google Earth; the images in the study areas have a spatial resolution of ~2–3 m or better. Near Mawiyngkhung, the fault trace lies along the east side of a deeply incised valley in which a large reservoir stands (Figs. 5A and 5B). To the north along the fault trace, as shown in Figures 5C and 5D, the Badapani-Tyrsad fault offsets a series of fluvial risers in a left-lateral sense, with the largest offset on the order of ~170 m. Although cultivation could have modified the original river channel geometry, we believe this effect to be minimal. Farms in the area are plowed manually or by farm animals, and the lack of modern machinery makes large-scale modification of landscape unlikely. We did not check this site in the field and the lack of age constraints on the offset risers prevents us from estimating the fault slip rate. However, by examining the global positioning system (GPS) velocity data of Jade et al. (2007) in the Shillong plateau region, we obtain ~5 mm/yr left-slip rate across the shear zone.

In addition to offset fluvial risers, we also notice the development of hairpin drainage geometry, the hallmark of active strike-slip faulting (Lacassin et al., 1998), across the Badapani-Tyrsad fault zone (Fig. 5E). Our interpretation that the Badapani-Tyrsad fault zone is a left-slip structure is also consistent with the left-lateral deflection of the Brahmaputra River directly north of the Mikir Hills (Fig. 2A). We believe that the Badapani-Tyrsad fault is only one of several northeast-striking left-slip faults across the Shillong Plateau. Another major left-slip fault zone appears to pass through the town of Guwahati, offsetting the northern margin of the Shillong Plateau and deflecting the Brahmaputra River channel left-laterally (i.e., the inferred Guwahati fault in Fig. 2A).

The northward extent of the Badapani-Tyrsad fault system is not clear, but we note that its projection follows approximately the rather linear northwestern edge of the Mikir Hills (Fig. 2A). Our interpreted left-slip kinematics also explain the apparent ~20 km of left-lateral offset of the northern edge of the Shillong Plateau (Fig. 2A). We examined the southern extension of the Badapani-Tyrsad fault via analysis of LAND-SAT images. The fault appears to terminate into a series of east-trending folds in the Cretaceous strata on the west side of the fault, with diminishing prominence in topographic expression as it approaches the Dauki thrust.

Although the contact between the basement and the Shillong Group is not exposed, we infer it to be a northwest-dipping thrust, placing the basement rocks over the Shillong Group strata. We made this interpretation for two reasons. First, our field observation demonstrates a rapid decrease in the magnitude of contractional deformation as expressed by a diminishing intensity of cleavage development and the tightness of folds in the Shillong Group away from the contact. Second, our U-Pb detrital zircon geochronologic work, as presented later in this study, raises the possibility that the strata of the Shillong Group directly against the basement contact are not the oldest part of the sequence; this implies that the basement contact is tectonic. The thrust interpretation is consistent with the observation that the contact is parallel to regional folds and foliation of contractional origin, as indicated by our mapping (Fig. 3A). We name this fault the Central Shillong thrust (CST, Figs. 2A and 3A).

Evans (1964) originally inferred the Dauki fault to be a major right-slip fault with >200 km of motion. However, the segment of the Dauki fault zone we examined ~12–14 km south of the Cheerapunjee is a thrust contact. In the field, the active fault trace can be clearly identified by its morphologic expression, which displays two levels of incised terrace surfaces in the hanging wall against a flat floodplain in the footwall. The fault zone along a road cut displays several minor imbricate thrusts in the Cretaceous strata, which strike N75–80ºE and dip 25–30ºN. All of the faults display downdip striations and thrust offsets.

Mikir Hills

We examined the northernmost Mikir Hills against the Brahmaputra River, where we identified three phases of plutonism. The first two phases are medium-grained biotite granite and coarse-grained K-feldspar augen gneiss, both containing gneissic foliation. The last phase is an undeformed K-feldspar–rich granitic dike that cuts the older deformed plutons (Fig. 4A). This relationship suggests that the last phase of pluton emplacement postdates regional development of the gneissic foliation.

Brahmaputra River Valley

Small outcrops of crystalline rocks up to 1–2 km in the longest dimension occur throughout the Brahmaputra River Valley. We examined several localities in the valley and found that the main lithologic units are foliated biotite granite, K-feldspar granite, and augen gneiss. The dominant strike of the foliation in the basement rocks is N15–30ºE, which is parallel to the dominant foliation trend in the Shillong Plateau and Mikir Hills. This relationship suggests a regional tectonic event that has transformed the original structural trends into a uniform northeast direction. As discussed in our U-Pb zircon dating section, this event was most likely associated with the 520–500 Ma collision between India and Antarctica, which produced the northeast-trending foliation, magmatism, and widespread metamorphic zircon growth. The widespread occurrence of the crystalline basement rocks across the Brahmaputra River Valley is unique in the Himalayan foreland basin and suggests that the foreland sediments are much thinner there than elsewhere in northern India (Gansser, 1983). It also suggests that the Brahmaputra River Valley may be mainly a piggyback basin of the Shillong uplift (Fig. 2B).

U-Pb ZIRCON GEOCHRONOLOGY OF CRYSTALLINE ROCKS

Methods

We conducted U-Pb spot dating on zircons from granitoid and orthogneiss samples from the Shillong Plateau, Mikir Hills, and the Brahmaputra River Valley using the Cameca 1270 ion microprobe at the University of California–Los Angeles (UCLA). The analytical procedure follows that of Quidelleur et al. (1997), and the analyses were conducted using an 8–15 nA O⁻ primary beam and an ~25-μm-diameter spot size. U-Pb ratios were determined using a calibration curve based on UO/U versus Pb/U from zircon standard AS3 (age 1099.1 Ma;
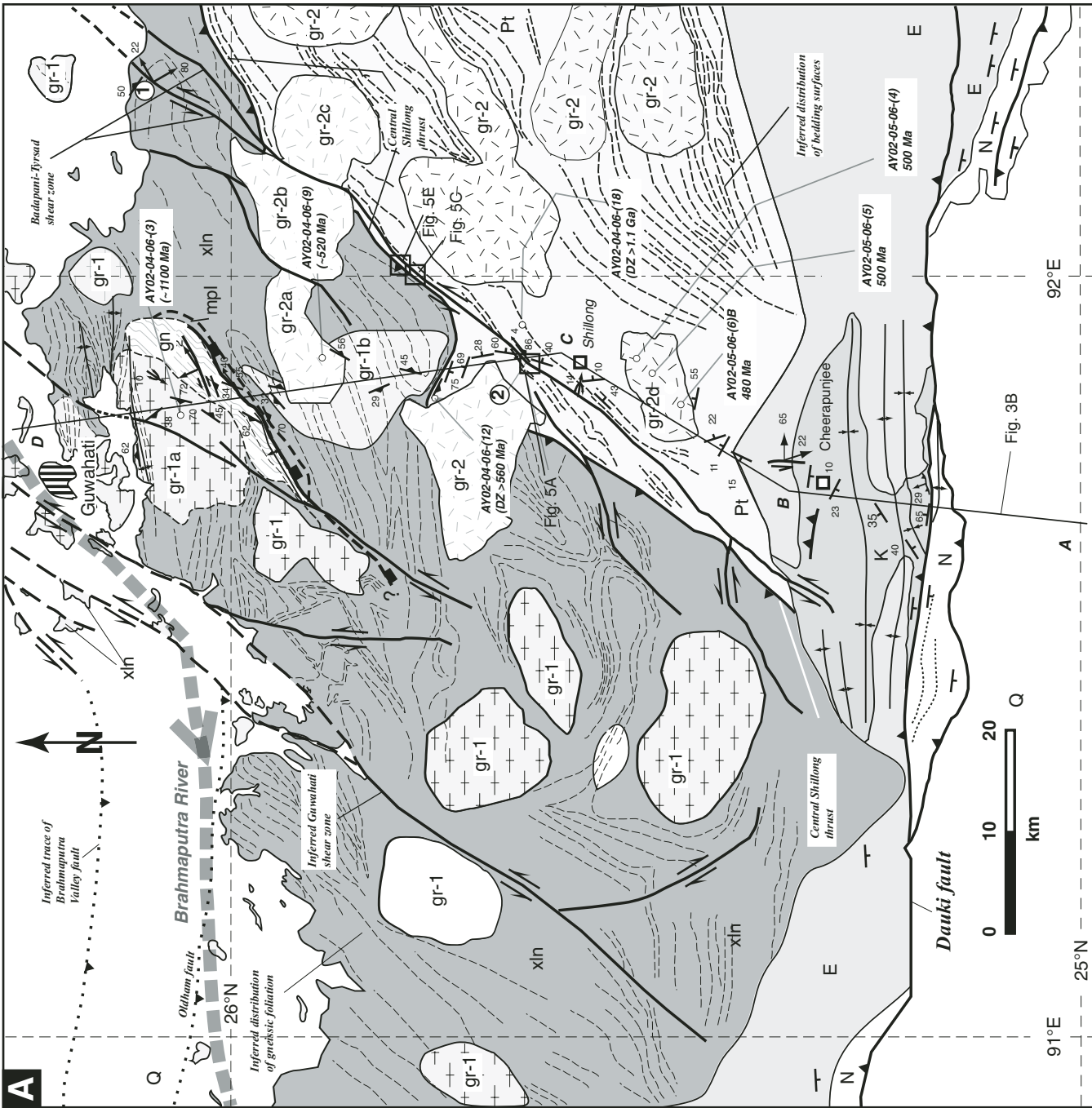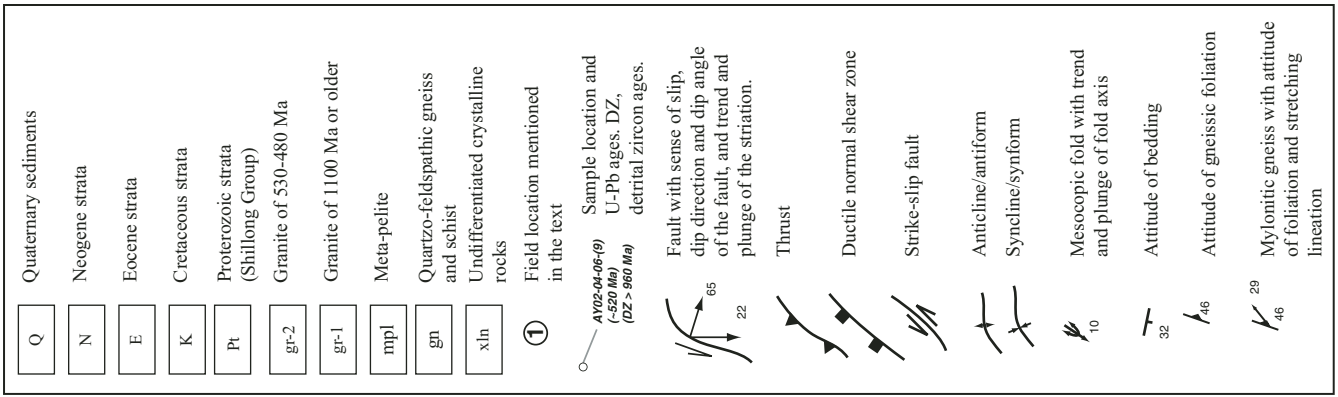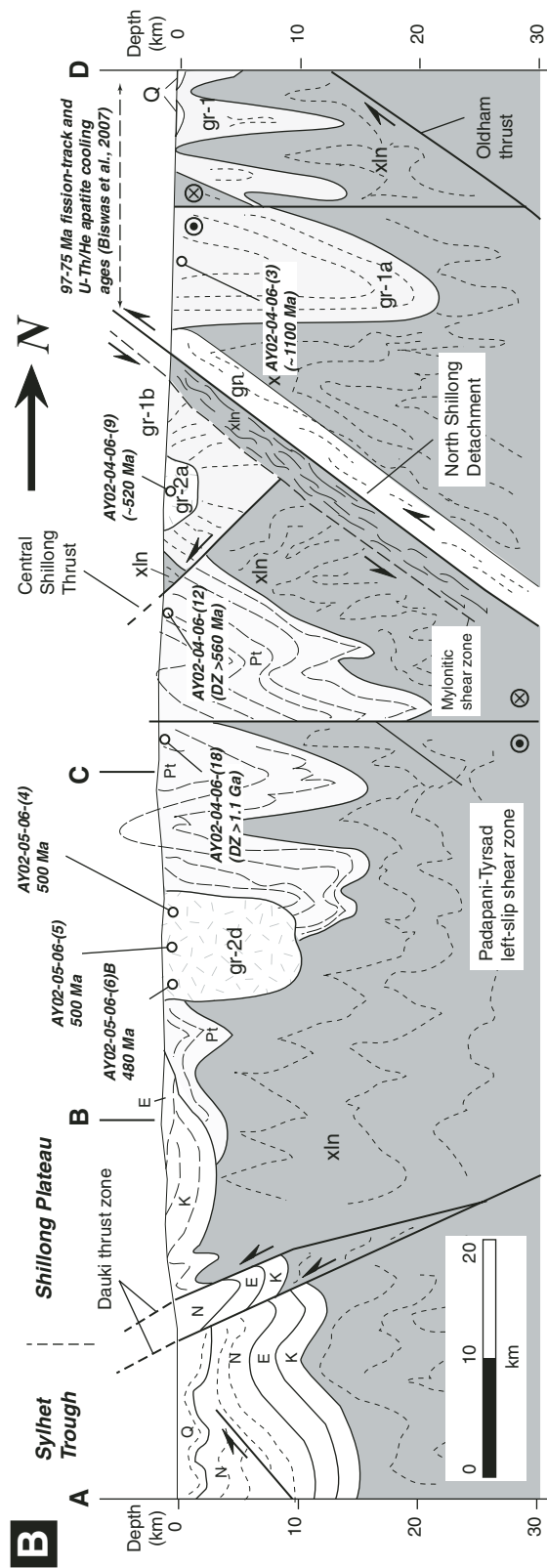
Figure 3 (*on this and previous page*). (A) Geologic map of the central Shillong Plateau based on our field mapping, interpretation of LANDSAT images, and a compilation of geologic maps from Srivastava et al. (2005) and Ghosh et al. (2005). Strikes and dips of foliation and bedding attitudes are from this study. Regional trends of bedding and foliations are interpreted from LANDSAT images. (B) Geologic cross section of the central Shillong Plateau. The depth to Moho is from Mitra et al. (2005).

Figure 4. Field pictures. (A) Undeformed 1084 Ma granitic dike (represented by sample AY01–03–05C) that intrudes into foliated orthogneiss in Mikir Hills (at location AY01–03–05 in Fig. 2A). (B) Eocene broadly folded coal-bearing sandstone, claystone, and siltstone exposed in the south-central Shillong Plateau. (C) Undeformed granite that intrudes the Proterozoic Shillong Group. (D) Thickly bedded quartz arenite of the Shillong Group that is intruded by undeformed early Paleozoic granitoid. (E) Flat-lying to gently south-dipping Cretaceous strata in the southern Shillong Plateau. (F) Isoclinal folds in the Shillong Group just outside the town of Shillong.
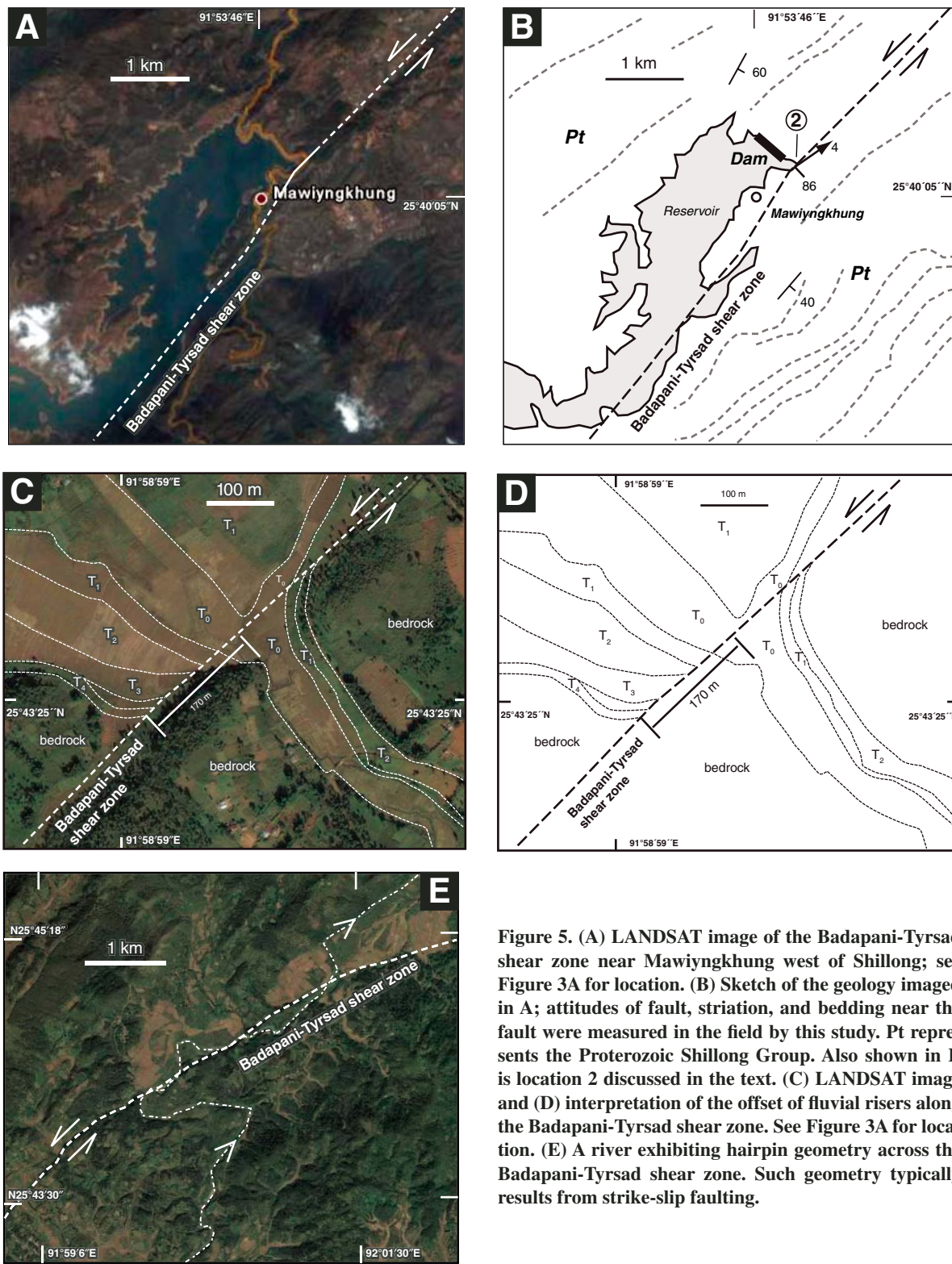
Figure 5. (A) LANDSAT image of the Badapani-Tyrsad shear zone near Mawiyngkhung west of Shillong; see Figure 3A for location. (B) Sketch of the geology imaged in A; attitudes of fault, striation, and bedding near the fault were measured in the field by this study. Pt represents the Proterozoic Shillong Group. Also shown in B is location 2 discussed in the text. (C) LANDSAT image and (D) interpretation of the offset of fluvial risers along the Badapani-Tyrsad shear zone. See Figure 3A for location. (E) A river exhibiting hairpin geometry across the Badapani-Tyrsad shear zone. Such geometry typically results from strike-slip faulting.

Yin et al.

Paces and Miller, 1993). We collected our data during four analytical sessions, each of which has a different calibration curve over distinct ranges in UO/U values (see notes in Table 1 in GSA Data Repository for the range of UO/U values[1]). We also adjusted isotopic ratios for common Pb corrections following Stacey and Kramers (1975). We calculated concentrations of U by comparison with zircon standard 91500, which has a U concentration of 81.2 ppm (Wiedenbeck et al., 2004). Data reduction was accomplished via the in-house program ZIPS 3.0.3 written by Chris Coath.

Results

Mikir Hills

We collected three samples from the same location along the northern rim of the Mikir Hills (Fig. 2). The samples represent three phases of plutonic emplacement. Sample AY 01–03–05-(1)A is from a foliated biotite granite, sample AY 01–03–05-(1)B is from a foliated K-feldspar granite that crosscuts the biotite granite, and sample AY 01–03–05-(1)C is from a K-feldspar granitic dike that is undeformed and intrudes the older deformed biotite and K-feldspar granites. We obtained eight spot ages on eight different zircon grains from sample AY 01–03–05-(1)A, which yielded $^{207}Pb/^{206}Pb$ ages ranging from 1039 Ma to 1129 Ma, with a weighted mean age of 1110 ± 15 Ma (2σ). We interpret the latter as the crystallization age of the oldest phase of granitoid at this location (Fig. 6).

We acquired 19 spot analyses on 16 zircon grains from sample AY 01–03–05-(1)B, which yielded three age ranges. One concordant group from six spot analyses has a $^{207}Pb/^{206}Pb$ weighted mean age of 1111 ± 42 Ma (2σ). Another concordant group from three spot analyses has a $^{207}Pb/^{206}Pb$ weighted mean age of 489 ± 34 Ma (2σ) with low Th/U ratios (Fig. 6) (Table 1 in GSA Data Repository, see footnote 1). Finally, ten spot analyses plot ages between the first two age groups. We cannot explain the high common Pb as an analytical problem because zircons from samples with low common Pb were prepared on the same probe mount and analyzed during the same session for the sample with high common Pb. It is possible that our analyzed zircons contain inclusions with high common Pb and some of our spots sampled these inclusions. The older age of 1111 ± 42 Ma (2σ) for sample AY 01–03–

05-(1)B is very similar to the weighted mean age for sample AY 01–03–05-(1)A, suggesting that the emplacement of the K-feldspar granite occurred immediately after the intrusion of the biotite granite. The low Th/U ratios of the younger age analyses from AY 01–03–05-(1)B (ca. 489 Ma) indicate later zircon growth during a metamorphic event.

Ten spot analyses on eight zircons from sample AY 01–03–05-(1)C yielded a $^{207}Pb/^{206}Pb$ weighted mean age of 1084 ± 19 Ma (2σ). Although this age is slightly younger than the average crystallization ages of the two deformed plutons described previously, the difference is within the 2σ confidence limit, and we do not consider it significant. Because of this, we can only broadly bracket the ductile deformation as expressed by gneissic foliation to have occurred ca. 1100 Ma.

We note that two analyses of sample AY 01–03–05-(1)C show significant discordance, plotting along a discordia line that may extend to the Phanerozoic (Fig. 6). Considering the results from sample AY 01–03–05-(1)B, this may represent the same metamorphic event at ca. 490 Ma.

Brahmaputra River Valley

Sample AY 02–07–06-(2) was collected from K-feldspar augen gneiss in an isolated basement outcrop north of the Mikir Hills and directly against the Brahmaputra River (Fig. 2). We did 14 spot analyses on 14 different zircon grains. Six reversely discordant analyses feature UO/U values beyond the range of calibration, as do four other analyses, such that only four remaining analyses are within the calibration range. The latter four analyses range in $^{207}Pb/^{206}Pb$ age from 1520 Ma to 1630 Ma (Fig. 7A). Most analyses yielded $^{207}Pb/^{206}Pb$ ages that span from 1400 to 1628 Ma. A single, dramatically reversely discordant analysis with a low Th/U ratio yields latest Proterozoic–early Paleozoic ages (the $^{238}U/^{206}Pb$ age is >400 m.y. older than the $^{207}Pb/^{206}Pb$ age). Using the four concordia analyses that have U concentration within the range of calibration, we interpret the augen gneiss to have crystallized broadly between 1520 Ma and 1630 Ma. The augen gneiss unit was affected by a later metamorphic event after the latest Proterozoic, which may correlate with the ca. 490 Ma event as detected in the northern Mikir Hills.

Shillong Plateau

In total, five samples from both deformed and undeformed plutonic rocks were analyzed across the Shillong Plateau. Sample AY 02–04–06-(3) was collected from a foliated biotite granite in the northernmost Shillong Plateau east of

Guwahati (unit gr-1a in Fig. 3A). We performed 16 spot analyses on 13 zircon grains for the sample and obtained ages from 500 Ma to 1600 Ma (Fig. 7B). Three concordant analyses cluster at ca. 500 Ma, and all have low Th/U ratios (0.032 and 0.137), suggesting a metamorphic origin (Table 1 in GSA Data Repository, see footnote 1) (Fig. 7C). Another concordant age cluster is at ca. 1100 Ma, and these are dominated by high Th/U ratios (mostly 1.1–1.4) (Table 1 in GSA Data Repository, see footnote 1), suggesting an igneous origin. Finally, two grains yielded concordant ages of 1521 ± 28 and 1598 ± 26 Ma and relatively high Th/U ratios of 0.573 and 0.183, indicating that they were derived from igneous rocks. There are three possible interpretations for the obtained ages. First, the granite crystallized at ca. 500 Ma and inherited various older igneous zircons of 1100–1600 Ma. Second, the granite crystallized at 1100 Ma with 1600 Ma inherited zircons. Third, the granite crystallized at 1600 Ma and experienced later zircon-growth events at 1100 Ma and 500 Ma, respectively. Because ca. 500 Ma concordant analyses are associated with low Th/U values, reflecting Pb loss and new zircon growth, and only two grains have ages of 1520–1600 Ma, we favor the second interpretation—that the dominant concordant ages clustered at 1100 Ma represent the crystallization age of the pluton. This interpretation implies that the 1100 Ma orthogneiss intruded into an older basement that contains 1600 Ma igneous zircons and the 1100 Ma orthogneiss and the older basement together experienced a later metamorphic event at ca. 500 Ma. It is possible that the 1600 Ma zircons were from a basement pluton emplaced during the same period as the one we dated in the Brahmaputra River Valley. This interpretation implies a regionally extensive magmatic event at 1600 Ma in northeastern India.

Sample AY 02–04–06-(9) was collected from an augen gneiss (gr-2a in Fig. 3A) that intrudes into the Shillong crystalline basement rocks and an older deformed granite (units xln and gr-1 in Fig. 3A). We conducted seven spot analyses on different zircon grains from the sample, which yielded a clustered age population around 520 Ma on the concordia plot (Fig. 7D). The zircons have high to moderate Th/U ratios (Table 1 in GSA Data Repository, see footnote 1), indicating an igneous origin. Some ages are slightly reversely discordant, so if these ages represent a single crystallization event, it must have occurred between the weighted mean $^{238}U/^{206}Pb$ age of 530 ± 7 Ma (2σ) and the mean $^{207}Pb/^{206}Pb$ age of 490 ± 9 Ma (2σ). This age estimate suggests that the gneissic foliation in the deformed granitoid was developed after 530 Ma. Despite the uncertainty, our U-Pb zircon age of this
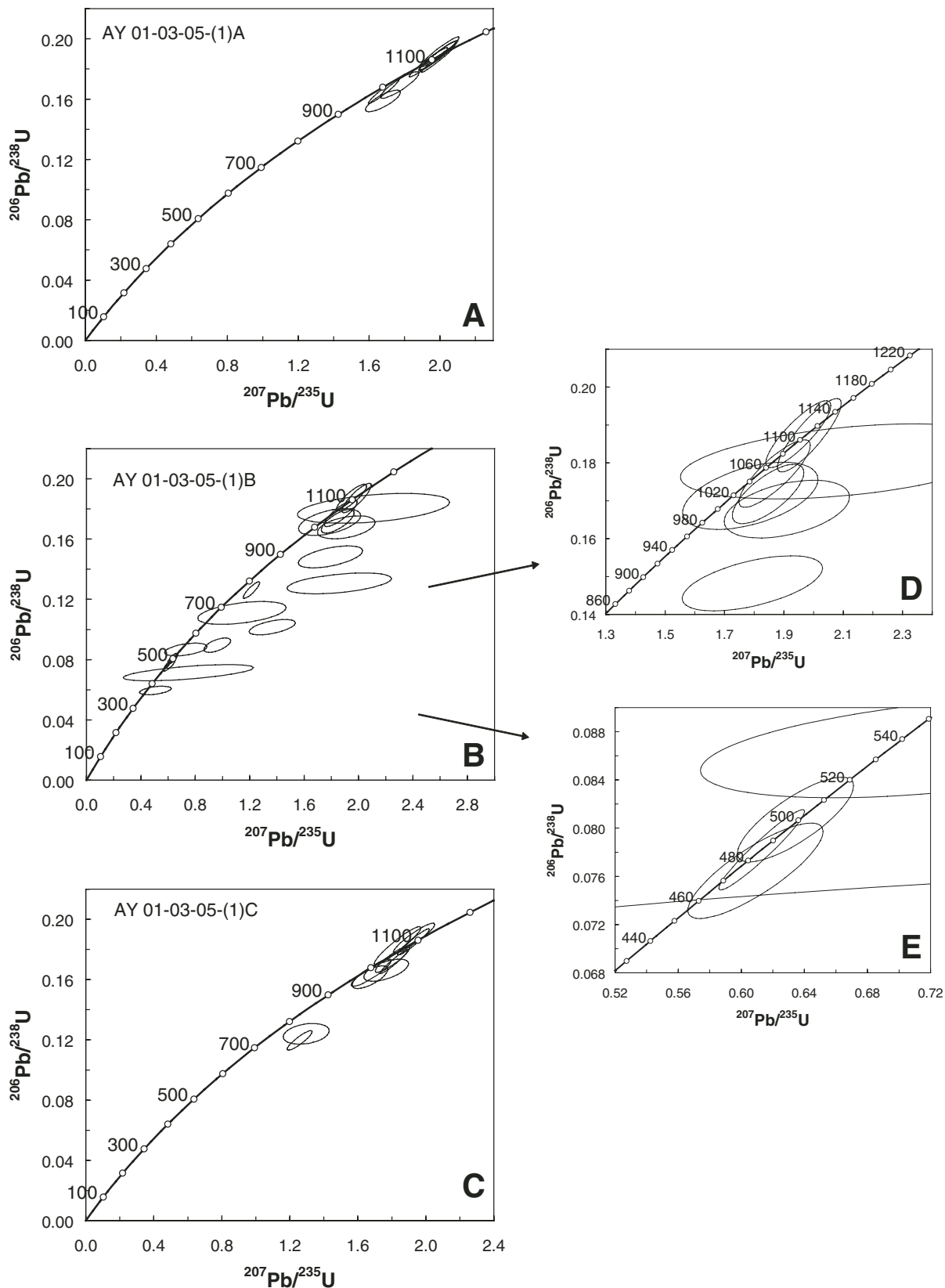
Figure 6. U/Th-Pb zircon concordia diagrams for samples collected from Mikir Hills. (A) Concordia diagram for sample AY 01–03–05-(1)A. (B) Concordia diagram for sample AY 01–03–05-(1)B. (C) Concordia diagram for sample AY 01–03–05-(1)C. (D–E) Blown-up concordia diagrams for sample AY 01–03–05-(1)B.
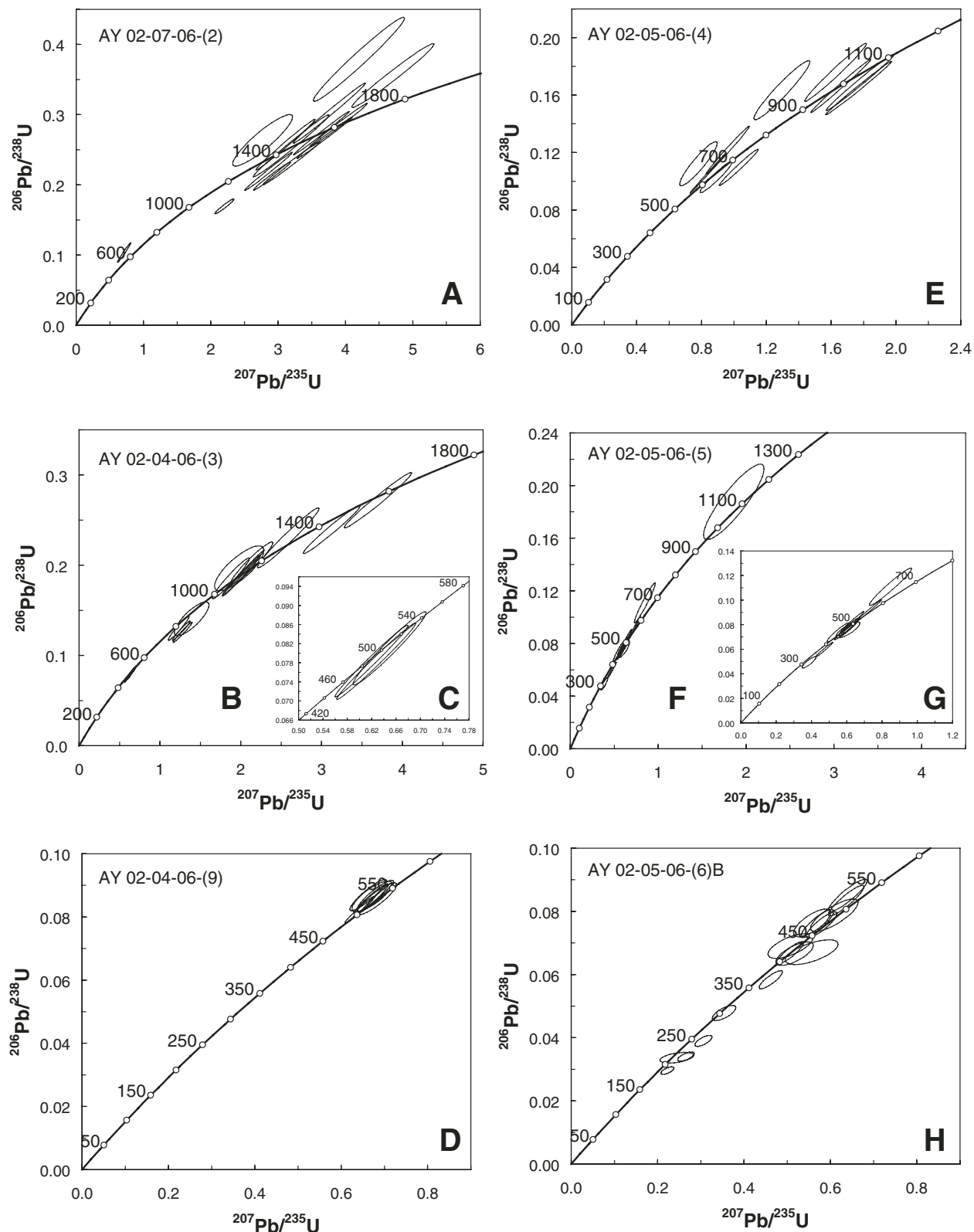
Figure 7. U-(Th)-Pb zircon concordia diagrams for samples collected from the Brahmaputra River Valley and Shillong Plateau. (A) Concordia diagram for sample AY 02–07–06-(2). (B) Concordia diagram for sample AY 02–04–06-(3). (C) Enlarged lower segment of concordia diagram for sample AY 02–04–06-(3). (D) Concordia diagram for sample AY 02–04–06-(9). (E) Concordia diagram for sample AY 02–05–06-(4). (F) Concordia diagram for sample AY 02–05–06-(5). (G) Enlarged lower concordia diagram for sample AY 02–05–06-(5). (H) Concordia diagram for sample AY 02–05–06-(6)B.

deformed pluton is significantly different from the Rb-Sr whole-rock isochron ages of 464 Ma and 550 Ma from the same deformed pluton (see summary by Ghosh et al., 2005) (Fig. 2A). This difference requires caution when using Rb-Sr ages to interpret the crystallization age of the plutons in the region.

In order to constrain the age of regionally extensive ductile deformation across the central Shillong Plateau and the age of the Shillong Group, we dated three samples (AY 02–05–06-[4], AY 02–05–06-[5], and AY 02–05–06-[6]B) from the same undeformed plutonic complex that intrudes the Shillong Group strata (unit gr-2d in Fig. 3A). Sample AY 02–05–06-(4) was collected from the northern margin of the granitoid, where it intrudes into the phyllite and quartzite of the Shillong Group (Fig. 4C). We performed single spot analyses on each of 10 zircon grains from the sample. Five of the analyses showed reverse discordance, four of them exhibited discordance, and one was concordant with an age of ca. 1000 Ma (Fig. 7E). All but one of the analyses have UO/U values below the range of the calibration. The discordant analyses define a lower intercept age of ca. 500 Ma. There are two possible interpretations for the obtained ages. The first is that the 1000 Ma concordant age may represent the time of crystallization for the pluton, which experienced a later thermal event at ca. 500 Ma. The second interpretation is that the pluton crystallized at ca. 500 Ma, incorporating inherited 1000 Ma zircons from the wall rocks, and the same 500 Ma emplacement event also caused Pb loss of the older zircons, resulting in their discordant ages. The two interpretations imply very different ages for the Shillong Group. That is, it is either older than ca. 1000 Ma, or older than ca. 500 Ma. The first interpretation would require parts of the Shillong Group to have been deposited in or prior to the middle Proterozoic.

Although we could not differentiate the two possibilities for sample AY 02–05–06-(4), we were able to obtain a crystallization age for sample AY 02–05–06-(5) from the central part of the same plutonic complex (Figs. 3A and 4C). For this sample, we obtained 11 analyses on seven zircon grains that display a relatively simple age pattern despite significant reverse and normal discordance (Figs. 7F and 7G). Analysis of one grain yielded an age of ca. 1100 Ma, and the rest have a weighted mean $^{207}Pb/^{206}Pb$ age of 497 ± 9 Ma (2σ). The discordance may be due to all but three of the analyses being beyond the calibration range. We interpret these results as indicating the pluton crystallized at ca. 500 Ma, with an inherited grain of ca. 1100 Ma.

Sample AY 02–05–06-(6)B was collected along the southern margin of the deformed pluton (unit gr-2d in Fig. 3A). This portion of the

granite intrudes into a thickly bedded quartz arenite sequence of the Shillong Group. We conducted 16 spot analyses from 13 zircon grains, with two spots on three of our analyzed zircons. On a concordia plot, the data appear to show a cluster of mostly concordant ages between 430 Ma and 480 Ma, with a potential discordia line extending down toward 100–120 Ma (Fig. 7H). These younger ages correspond well to the age range of Cretaceous igneous activities at 105–115 Ma in the southern Shillong Plateau (e.g., Lal et al., 1978; Srivastava and Sinha, 2004a, 2004b; Srivastava et al., 2005). We interpret the early Paleozoic age cluster at 430–480 Ma to represent the crystallization age of the undeformed pluton, followed by a Pb-loss event in the Cretaceous. The crystallization age inferred from sample AY 02–05–06-(6)B is slightly younger than that constrained by samples AY 02–05–06-(4) and AY 02–05–06-(5) at ca. 500 Ma, indicating a possible diachronous emplacement of this large plutonic complex.

We note that the plutonic complex we dated using samples AY 02–05–06-(4), AY 02–05–06-(5), and AY 02–05–06-(6)B (unit gr-2d in Fig. 3A) previously yielded a Rb-Sr age of ca. 600 Ma as summarized in Ghosh et al. (2005). This age is significantly different from our result and again suggests caution when using the Rb-Sr ages to interpret crystallization age of the plutons in the region.

In summary, our U-Pb zircon dating of five samples indicates that the Shillong Plateau exposes plutonic rocks emplaced at ca. 1100 Ma and 520–430 Ma, respectively. The pre–1100 Ma basement contains 1600 Ma igneous zircons, which may correlate with the 1600 Ma orthogneiss in the Brahmaputra River Valley. The crosscutting relationships bracket portions of the Shillong Group to predate 430–500 Ma. The U-Pb zircon dating also constrains the regional gneissic foliation and isoclinal folds in the Shillong Group to have occurred between 520 Ma (youngest deformed granite) and 500 Ma (oldest undeformed granite). Although these constraints on the age of the Shillong Group are broadly consistent with the Proterozoic age assignment (Das Gupta and Biswas, 2000), the initial age of deposition for the sequence is unknown. We address this issue next by presenting U-Pb detrital zircon ages of the Shillong Group.

U-Pb DETRITAL ZIRCON GEOCHRONOLOGY OF CRYSTALLINE ROCKS

Method

We conducted U-Pb dating of detrital zircons from two samples of the Shillong Group, sam-

ples AY 02–04–06-(12) and AY 02–04–06-(18) (see Fig. 3A for locations). Zircon grains from each sample were set in an epoxy and mounted adjacent to several reference standard zircon crystals. We performed U-Pb geochronology on zircons using laser-ablation–multicollector–inductively coupled plasma–mass spectrometry (LA-MC-ICP-MS) at the LaserChron Center of the University of Arizona. The analyses involved ablation of zircon with a New Wave DUV193 Excimer laser operating at a wavelength of 193 nm and using a spot diameter of 15–35 μm. The ablated material is carried in helium into the plasma source of a GVI Isoprobe, which is equipped with a flight tube of sufficient width that U, Th, and Pb isotopes are measured simultaneously. We made all measurements in a static mode using Faraday detectors for ^{238}U, ^{232}Th, $^{208-206}Pb$, and an ion-counting channel for ^{204}Pb. Ion yields were ~1.0 mv per ppm. Each analysis consisted of one 20 s integration on peaks with the laser off (for backgrounds), twenty 1 s integrations with the laser firing, and a 30 s delay to purge the previous sample and prepare for the next analysis. The ablation pit was ~15 μm in depth.

For each analysis, the measurement uncertainty in determining $^{206}Pb/^{238}U$ and $^{206}Pb/^{204}Pb$ was ~1%–2% (2σ) in the $^{206}Pb/^{238}U$ age. The measurement uncertainties of $^{206}Pb/^{207}Pb$ and $^{206}Pb/^{204}Pb$ were also ~1%–2% (2σ) for ages older than 1.0 Ga, but uncertainty was substantially larger for younger grains due to low intensity of the ^{207}Pb signal. For most analyses, the crossover in precision of $^{206}Pb/^{238}U$ and $^{206}Pb/^{207}Pb$ ages occurred at 0.8–1.0 Ga.

We corrected common Pb by using the measured ^{204}Pb and assuming an initial Pb composition from Stacey and Kramers (1975) (with uncertainties of 1.0 for $^{206}Pb/^{204}Pb$ and 0.3 for $^{207}Pb/^{204}Pb$). Our measurement of ^{204}Pb was unaffected by the presence of ^{204}Hg because backgrounds were measured on peaks (thereby subtracting any background ^{204}Hg and ^{204}Pb), and because very little Hg was present in the argon gas.

Interelement fractionation of Pb/U is generally ~20%, whereas fractionation of Pb isotopes is generally ~2%. In-run analysis of fragments of a large zircon crystal (generally every fifth measurement) with known age of 564 ± 4 Ma (2σ) was used to correct for this fractionation. The uncertainty resulting from the calibration correction was generally 1%–2% (2σ) for both $^{206}Pb/^{207}Pb$ and $^{206}Pb/^{238}U$ ages. Interpreted ages are based on $^{206}Pb/^{238}U$ for grains younger than 800 Ma grains and on $^{206}Pb/^{207}Pb$ for grains older than 800 Ma. Analyses that were >30% discordant (by comparison of $^{206}Pb/^{238}U$ and $^{206}Pb/^{207}Pb$ ages) or >5% reverse discordant

were not considered further. All analytical data are listed in Table 2 in GSA Data Repository (see footnote 1).

Results

Sample AY 02–04–06-(12) was collected from a quartz arenite unit directly east of the contact between the Shillong Group and crystalline basement (Fig. 3A). This sample yielded two dominant age populations, one between 900 Ma and 1150 Ma and another between 1450 Ma and 1850 Ma (Figs. 8 and 9). These age clusters correspond well to the crystallization ages of orthogneiss units in the Shillong Plateau, Mikir Hills, and Brahmaputra River Valley described earlier, suggesting that they are probably derived from a local source. There are also two minor age groups at 560 Ma and 2500 Ma. Deciphering whether the young zircon grains with 560 Ma ages are metamorphic or igneous is critical in interpreting the age of the Shillong Group and the tectonic setting for its deposition. Because the young grains have low U/Th ratios of 1.0 and 1.5 (Table 2 in GSA Data Repository, see footnote 1), respectively, we interpret them to have an igneous origin. Thus, the deposition age of this portion of the Shillong Group must be younger than ca. 560 Ma.

Sample AY 02–04–06-(18) was collected from a sandstone unit near the town of Shillong. Because Shillong Group strata are isoclinally folded, the stratigraphic relationship between this sample and the first sample discussed above is not clear. We analyzed 97 zircon grains from this sample that yielded Pb-Pb ages from 1100 Ma to 3300 Ma (Fig. 8). The ages mainly fall into two groups between 1100 Ma and 1250 Ma and between 1500 Ma and 1750 Ma. The age distribution of this sample is similar to that for sample AY 02–04–06-(12) in that they both have the 1600–1700 Ma age peaks. However, the sample differs from the first sample by its lack of 560 Ma zircons and the slightly older 1200 Ma peak compared to the age cluster at 900–1100 Ma age (Figs. 8 and 9).

In summary, the detrital zircon ages indicate that the Shillong Group received sediments from 1200 to 1100 Ma plutonic rocks and an earlier basement that contains ca. 1600 Ma zircons. Deposition of sample AY 02–04–06-(12) postdated ca. 560 Ma, while deposition of sample AY 02–04–06-(18) postdates 1100 Ma.

DISCUSSION

Our mapping documents the presence of a north-northeast–trending ductile normal shear zone with a top-to-the-southeast sense of shear in the northern Shillong Plateau. Our work also documents active left-slip faulting on the previously recognized northeast-striking Badapani-Tyrsad fault zone. Combined field observations and U-Pb zircon geochronology of deformed and undeformed granitoids indicate occurrence of ductile deformation, magmatism, and metamorphic zircon growth at ca. 1100 Ma and ca. 530–480 Ma, respectively. In the following discussion, we present the broader implications of these findings.

Proterozoic to Cambrian-Ordovician Magmatism

Our U-Pb zircon dating reveals three episodes of granitoid magmatism in northeastern India at ca. 1600 Ma, ca. 1100 Ma, and ca. 500 Ma. The discrete nature of the magmatic events is also indicated by the similar age clusters of detrital zircon from the Shillong Group at 900–1150 Ma and 1500–1750 Ma (Fig. 8).

Previous geochronologic work based on the Rb-Sr whole-rock isochron method had revealed a wide range of ages from ca. 1700 Ma to 420 Ma for orthogneiss and plutons in the Shillong Plateau and Mikir Hills (see summary by Ghosh et al., 2005). Although there are overlaps between the Rb-Sr ages and our newly acquired U-Pb zircon ages, our work does not indicate protracted magmatism between 800 Ma and 600 Ma (Fig. 8). We suspect that Neoproterozoic to Cambrian-Ordovician magmatism occurred during a much narrower age range, and the semicontinuous igneous activity as previously shown by Ghosh et al. (2005) was largely due to the lack of precision in the Rb-Sr method and its inability to detect multiple thermal events. The absence of detrital zircon ages from 900 Ma to 600 Ma in one sample from the Shillong Group is consistent with the lack of 800–600 Ma magmatism in the region, while the presence of 800–600 Ma zircons in other samples may have been derived from remote sources exotic to the Indian craton.

We note that the three episodes of magmatism as inferred from our U-Pb zircon dating are remarkably consistent with the three metamorphic events detected by chemical dating of metamorphic monazites from the metamorphic basement of the Shillong Plateau at 1600–1400, 1000–1300, and ca. 500 Ma, respectively (Chatterjee et al., 2007). This correlation suggests that magmatism and metamorphism were coeval.

As shown in Yin et al. (2009), the eastern Himalaya exposes augen gneisses with a narrowly defined U-Pb age of ca. 1745 Ma. This age was not detected by our work, but we note that Ameen et al. (2007) obtained a sensitive high-resolution ion microprobe (SHRIMP) zircon $^{207}Pb/^{206}Pb$ age of 1772 ± 6 Ma from basement rocks ~60 km west of the Shillong Plateau (see Fig. 2 for sample location). Thus, the lack of 1745 Ma orthogneiss in our study could simply be a result of the small number of dated samples.

Age of the Shillong Group and its Basement Rocks

The U-Pb zircon ages of 480–500 Ma from an undeformed pluton intruding the Shillong Group place an upper age bound for its deposition. That is, the youngest component of the Shillong Group must have been deposited between 560 Ma (the youngest detrital zircon ages for sample AY 02–04–06-[12]) and 500 Ma (the oldest zircon age for the crosscutting pluton). However, these age relationships do not preclude the existence of much older stratigraphic sections in the Shillong Group, particularly for the stratigraphic horizons at or below the position where sample AY 02–04–06-(18) was collected. That is, the deposition age of sample AY 02–04–06-(18) could be significantly older than sample AY 02–04–06-(12), even though the former is farther from the contact between the crystalline basement and the Shillong Group. We made this interpretation because sample AY 02–04–06-(18) lacks both the 900 Ma and 560 Ma zircons that were detected in sample AY 02–04–06-(12). Because sample AY 02–04–06-(18) is located only ~12 km away from sample AY 02–04–06-(12), the lack of zircon grains older than 900 Ma may imply that its deposition occurred prior to this age. This interpretation has major implications for determining the nature of the contact between the Shillong crystalline basement and the nearby Proterozoic Shillong Group. If the contact is presently depositional, then the oldest sedimentary sequence should lie directly above the contact, and the younger stratigraphic sections should be exposed away from the contact, which is inconsistent with our interpreted age distribution for the Shillong Group as discussed already. Thus, the contact between the basement and the Shillong Group is likely a fault, as indicated by our independent field observations.

Of course, the absence of younger zircons could also be explained by the sample size, which may have missed this minor component as shown by the small number of grains in sample AY 02–04–06-(12). For the latter case, the entire Shillong Group may all have deposited after 560 Ma but before 500 Ma, bracketing its total deposition time to be within ~60 m.y. Mitra and Mitra (2001) suggested that the lower part of the Shillong Group was deposited prior to 1550 Ma based on the Pb-Pb age of galena mineralization. This age constraint combined with ours would make the total duration of deposition of the Shillong Group ~1000 m.y., which
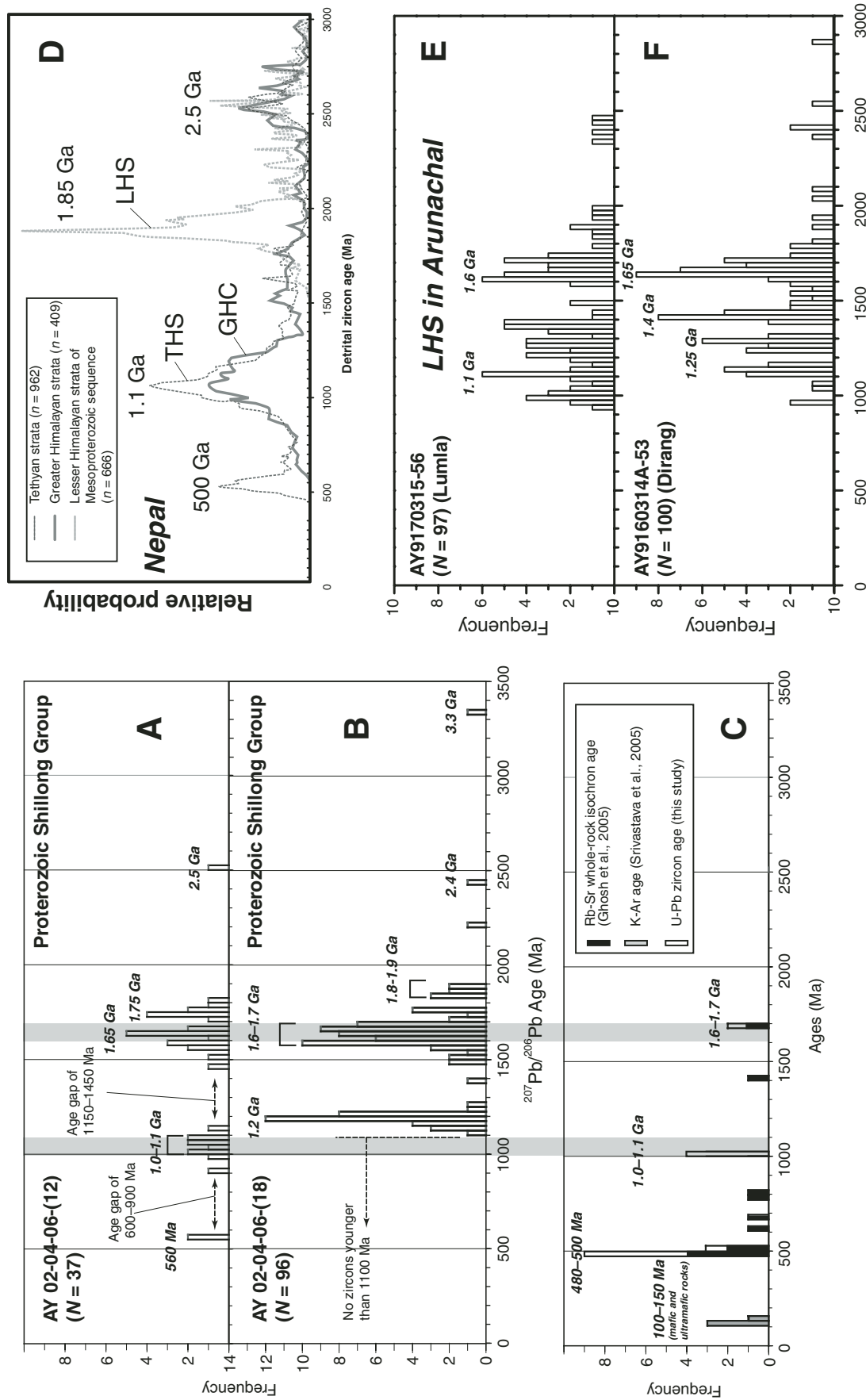
Figure 8. (A) Detrital zircon ages for sample AY 02–04–06–(12) from the Shillong Group. See Figure 3A for location. (B) Detrital zircon ages for sample AY 02–04–06–(18) collected from the Shillong Group. See Figure 3A for location. (C) Ages of igneous rocks from the Shillong Plateau, Mikir Hills, and Brahmaputra River Valley. Rb-Sr whole-rock isochron ages are from Ghosh et al. (2005) for igneous rocks from the Shillong region. Ages of mafic and ultramafic rocks are from Srivastava and Sinha (2004a, 2004b), and U-Pb zircon ages are from this study. (D) Detrital zircon ages of Himalayan units from Nepal after Gehrels et al. (2003). (E–F) Detrital zircon ages of Lesser Himalayan Sequence (LHS) from the Arunachal Himalaya after Yin et al. (2006). See Figure 2A for sample locations. THS—Tethyan Himalayan Sequence, GHS—Greater Himalayan Crystalline Complex.

Figure 9. Concordia plots of detrital zircon ages of for samples AY 02–04–06-(12) and sample AY 02–04–06-(18).

appears to be too long and is not consistent with the fact that a major tectonic event occurred ca. 1100 Ma during the propos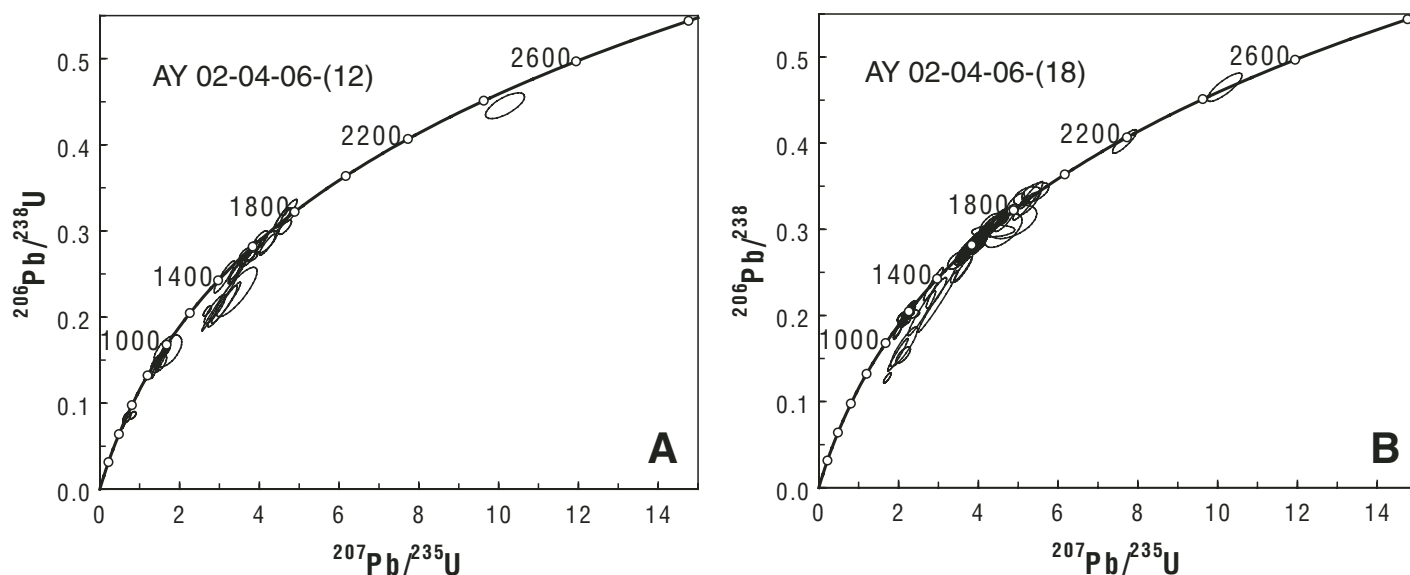ed period of deposition of the Shillong Group. In our opinion, the age of the Shillong Group is most likely younger than 900 Ma (the youngest zircon age in AY 02–04–06-[18]) and older than 530 Ma (the oldest granite that intrudes into the Shillong Group). This interpretation implies that the ca. 1100 Ma and ca. 1600 Ma orthogneiss units and the metasedimentary rocks they intrude into constitute the basement of the NE Indian craton overlain by the Proterozoic Shillong Group. As we did not observe the base of the Shillong Group, we cannot rule out its lowermost section to have been deposited in the Paleoproterozoic.

Age of the Central Shillong Thrust and Regional Contractional Deformation

The age of the Central Shillong thrust can be inferred from the age of the Shillong Group and a crosscutting pluton. Since the thrust cuts the part of the Shillong Group that contains 560 Ma detrital zircons, its motion must postdate this age (Fig. 3A). Because a plutonic complex consisting of three intrusive units intrudes the thrust (gr-2a, gr-2b, and gr-2c in Fig. 3A), the thrust motion predates the pluton. The westernmost part of this plutonic complex is made up of gneissic foliation and yields a U-Pb zircon age of ca. 520 Ma from sample AY 02–04–06-(9) (Fig. 3A). This crosscutting relationship suggests that motion on the Central Shillong thrust must predate 520 Ma, but the continuous ductile deformation producing gneissic foliation in the pluton lasted after 520 Ma. The upper age of the

regional contractional deformation can be constrained by the 500–480 Ma undeformed pluton that we dated in the southern Shillong Plateau (gr-2d in Fig. 3A). These observations suggest that motion on the inferred Central Shillong thrust occurred after 560 Ma but before 520 Ma, and regional ductile contractional deformation producing gneissic foliation and isoclinal folds occurred between 520 Ma and 500 Ma.

We note that early Paleozoic deformation has also been documented in the Himalayan orogen. From the crosscutting relationships and the ages of deformed and undeformed granitoids in the Nepal Himalaya, Gehrels et al. (2006a, 2006b) showed that north-south ductile contractional deformation occurred between 484 Ma and 474 Ma in the Dadeldhura thrust sheet in far-west Nepal and between 484 Ma and 473 Ma in the Kathmandu Nappe in south-central Nepal. Early Paleozoic high-grade metamorphism, possibly associated with the same contractional event, was also detected by U-Th/Pb dating of monazite inclusions in garnets from Greater Himalayan Crystalline Complex units in the Nepal Himalaya (Catlos et al., 2002; Kohn et al., 2004, 2005; Martin et al., 2007) and Sm-Nd dating of garnets in the NW India Himalaya (Argles et al., 1999). Combining the results from the Himalaya and the Shillong Plateau, we conclude that the northern and eastern margins of India experienced widespread contractional deformation in the Cambrian-Ordovician, possibly related to the amalgamation of the Eastern Gondwana supercontinent during the Pan-African event (e.g., Meert, 2003; Collins and Pisarevsky, 2005).

The Shillong Plateau is located north of the 1100–900 Ma, northwest-trending Eastern Ghats

orogen, which was considered to be produced by India-Antarctica collision during formation of the ca. 1100-Ma Rodinia supercontinent (Moores, 1991; Dalziel, 1991; Hoffman, 1991; Li et al., 2008). Specifically, the high-grade rocks of the Eastern Ghats belt of India have been correlated with the Napier and Rayner Complexes of Antarctica (e.g., Shaw et al., 1997; Mezger and Cosca, 1999; Boger et al., 2000; Kelly et al., 2002). The orogen later experienced magmatism and contraction between 550 Ma and 500 Ma during the amalgamation of Eastern Gondwana (Ghosh et al., 2004; Collins et al., 2007; Biswal et al., 2007). The similarities in deformation and magmatic history of the Eastern Ghats Belt and the Shillong Plateau suggest that the 1100 Ma and 550–500 Ma orogenic belts extend along the entire eastern margin of the Indian subcontinent.

Correlation and Comparison of Lithologic Units between the Himalaya and NE India

The U-Pb zircon ages of orthogneiss and granitoids and the general age constraint on the deposition of the Shillong Group allow us to compare lithologic units from the eastern Himalaya and northeastern India (Fig. 10). Richards et al. (2006) and Yin et al. (2009) showed that the Greater Himalayan Crystalline Complex includes orthogneiss with a U-Pb zircon age of ca. 820–880 Ma. Orthogneiss of this age has not been detected by this study in NE India, but this could be an artifact of our small sample size. The Greater Himalayan Crystalline Complex in Bhutan contains detrital zircons with U-Pb ages ranging from 980 Ma to 1820 Ma (Richards et
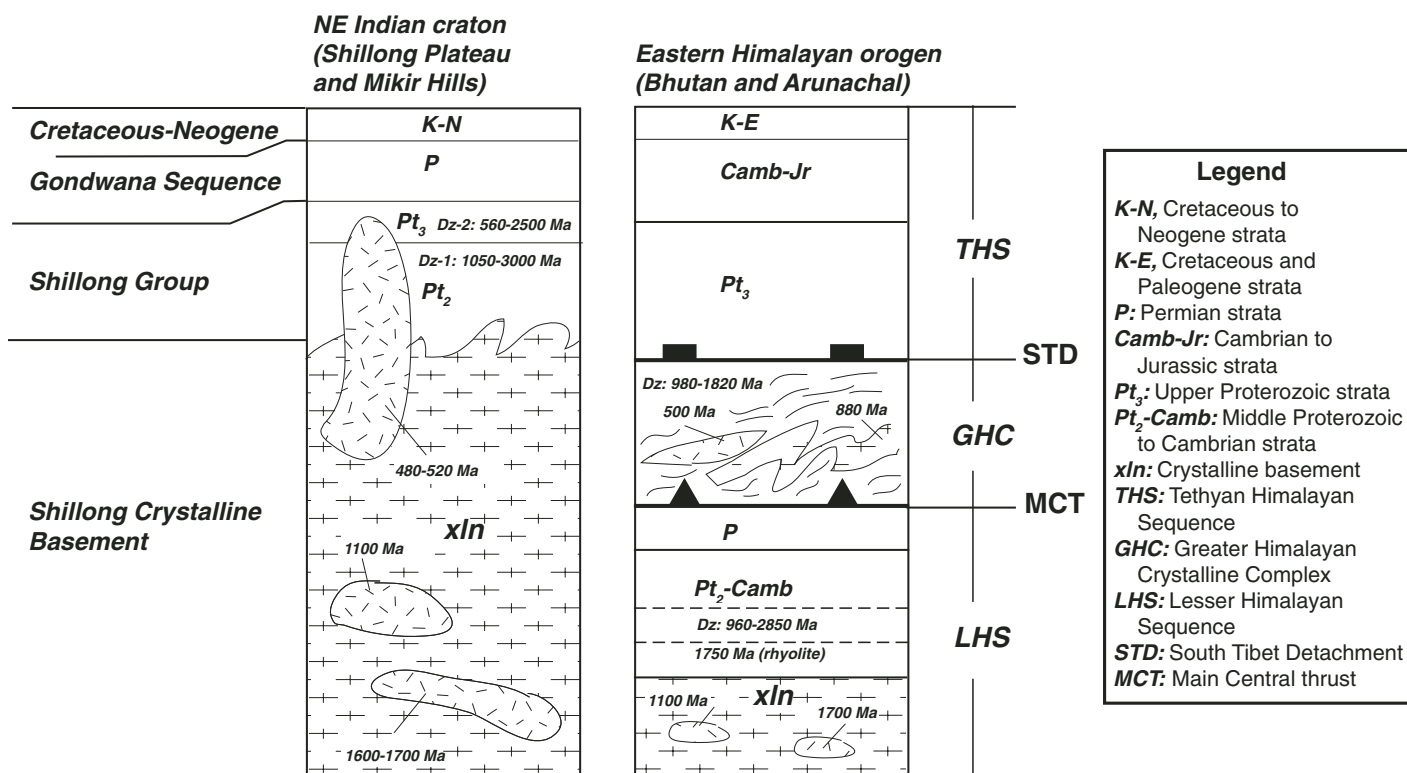
Figure 10. Correlation of lithostratigraphic units between the Himalaya and northeastern India. The age assignment of northeastern Indian units is based on the work of Das Gupta and Biswas (2000) and this study. The age assignment of the Himalayan lithologic units is based on the work of Kumar (1997), Tewari (2001), Richards et al. (2006), and Yin et al. (2006).

al., 2006) and is similar to that for sample AY 02–04–06-(18) from the Shillong Group in NE India. In Nepal, the Greater Himalayan Crystalline Complex is intruded by orthogneiss with ages between 520 Ma and 480 Ma and contains 1100 Ma detrital zircons. This age range is similar to that for the Shillong Group. This correlation implies that the protolith of the Greater Himalayan Crystalline Complex in the Himalaya may be similar to the Shillong Group and intruded 500 Ma orthogneiss.

In the Arunachal Himalaya, Kumar (1997) inferred the presence of 1900–1650 Ma orthogneiss in the Lesser Himalayan Sequence (LHS) based exclusively on Rb-Sr ages. Our work from the same area broadly confirms this result with crystallization ages tightly constrained to be ca. 1700 Ma (see detailed discussion in Yin et al., 2009). Also based on a Rb-Sr age, Bhargava (1995) inferred the presence of 1100 orthogneiss in the Bhutan Lesser Himalayan Sequence. Except in Bhutan, the 1100 Ma orthogneiss has not been documented in the Himalaya, although detrital zircons with this age are present in the Greater Himalayan Crystalline Complex and Tethyan Himalayan Sequence in Nepal and the Greater Himalayan Crystalline Complex and Lesser Himalayan Sequence in the eastern

Himalaya (DeCelles et al., 2000; Gehrels et al., 2003; Richards et al., 2006; Yin et al., 2006). This observation indicates that the 1100 Ma zircons in the Himalayan units did not occur in situ but were transported mostly from a source outside the Himalayan Range. We suggest that the Eastern Ghats orogen was the source of 1100 Ma zircons in the Himalayan units.

The detrital zircon ages from the Arunachal Himalaya range from 960 Ma to 3000 Ma (Figs. 8E and 8F). The presence of microfossils indicates that the uppermost part of the Lesser Himalayan Sequence in Arunachal has a Neoproterozoic–early Cambrian age (Tewari, 2001; Azmi and Paul, 2004). The detrital age distribution differs from the age distribution for the Lesser Himalayan Sequence in Nepal in that it contains zircons younger than 1500 Ma (Fig. 8D). Although the detrital zircons from both the Shillong Group and the Arunachal Lesser Himalayan Sequence display age clusters at ca. 1100 Ma and 1600–1700 Ma, the Arunachal zircons do not have the prominent age gap between 1200 Ma and 1500 Ma as seen in the Shillong Group samples.

The sedimentary strata of the Lesser Himalayan Sequence in Bhutan are interlayered either tectonically or depositionally with 1750 Ma

metarhyolite (Richards et al., 2006), which has not been detected from the Shillong Group. Detrital zircon from the Bhutan Lesser Himalayan Sequence units exhibits three age patterns (McQuarrie et al., 2008). The first is a continuous age distribution between 1000 Ma and 1700 Ma, similar to those from the Arunachal Lesser Himalayan Sequence units. The second is characterized by the presence of 500–600 Ma detrital zircon. The third type contains 500–600 Ma zircons but lacks 1000–1700 Ma zircon. The presence of 500–600 Ma detrital zircon and the absence of 1000–1700 Ma zircon are characteristic of detrital zircon age distributions for the Shillong Group. This comparison suggests that although differences exist, there is considerable overlap in age distribution between detrital zircons from the eastern Himalayan Lesser Himalayan Sequence and the Shillong Group in the northeastern Indian craton suggesting that the two areas were depositionally linked.

The Tethyan Himalayan Sequence (THS) in the Bhutan Himalaya has depositional ages ranging from the late Proterozoic–Cambrian to the Cretaceous (Bhargava, 1995). That is, the lowermost Tethyan Himalayan Sequence has a similar age to the uppermost Lesser Himalayan Sequence in the eastern Himalaya (Tewari,

2001). Detrital zircon from the late Proterozoic Tethyan Himalaya Sequence unit yields a prominent age cluster at ca. 900 Ma and minor clusters at 1500–1700 Ma and 2400–2500 Ma (McQuarrie et al., 2008). This age distribution is distinctively different from those of the Lesser Himalaya Sequence in the eastern Himalaya. Because only one sample has been analyzed so far from the Tethyan Himalaya Sequence in the eastern Himalaya (McQuarrie et al., 2008), it is not clear if different age distributions between the Tethyan Himalaya Sequence and Lesser Himalaya Sequence are simply a result of incomplete sampling.

The presence of 1600–1700 Ma (Richards et al., 2006) and possibly 1100 Ma (Bhargava, 1995) orthogneiss units in the Lesser Himalaya Sequence of the eastern Himalaya and NE India suggests that both regions may have shared the same crystalline basement belonging to the Indian craton. Despite some detailed differences, the presence of age clusters at 1100 Ma and 1600–1700 Ma for both the Lesser Himalaya Sequence in the eastern Himalaya and the Shillong Group suggests that they might be the same cover sequence originally on top of the basement that includes the 1600 Ma and 1100 Ma orthogneiss. Correlation of the 500 Ma plutons in the Shillong Plateau region and those common in the Greater Himalaya Crystalline Complex suggests that the Greater Himalaya Crystalline Complex may have also been derived from the Indian craton, since its pre-Cenozoic geology is similar to that exposed in the Shillong Plateau. First, widespread 500 Ma orthogneiss in the Himalaya may correlate with those in the Shillong region. Second, the age range of the metasedimentary rocks in the Greater Himalaya Crystalline Complex is quite similar to that for the Shillong Group. Finally, as discussed in Yin et al. (2009), the Greater Himalaya Crystalline Complex in the eastern Himalaya also contains orthogneiss with U-Pb zircon ages of 1700 Ma, further supporting origination of the Greater Himalaya Crystalline Complex from either the Indian craton or a separated terrane, as proposed by DeCelles et al. (2000), that has a similar Mesoproterozoic basement to that of northeastern India. Recent work by Murphy (2007) has shown that the structurally defined Greater Himalaya Crystalline Complex rocks above the Main Central thrust exposed in northern Himalayan gneiss domes have Nd isotopic compositions of Lesser Himalaya Sequence rocks. Since the Lesser Himalaya Sequence rocks can be clearly correlated with Indian cratonal rocks (DeCelles et al., 2000), it is likely that the Greater Himalaya Crystalline Complex basement correlative to the Lesser Himalaya Sequence is mostly buried in the northern Himalayan Range.

Cretaceous(?) Ductile Normal Shear Zone

The extensional kinematics of the North Shillong Detachment are drastically different from the widespread contractional structures in the region. There are two possible tectonic events that may have caused the observed extensional deformation in northeastern India: (1) the development of a passive continental margin in the late Proterozoic around the Indian continent prior to ca. 500 Ma orogenic event (e.g., Collins and Pisarevsky, 2005), or (2) Cretaceous breakup of the Gondwana (e.g., Srivastava et al., 2005; Ghosh et al., 2005). For the first interpretation, the ductile shear zone should have formed during the deposition of the Shillong Group and would predate the regional compression as represented by the development of regional gneissic foliation and related northeast-trending folds. The older age of the shear zone, compared to the contractional event, would require the shear zone to be folded during the ca. 500 Ma compressional event. However, our field observation indicates that the ductile shear zone postdates folding and regional development of gneissic foliation. This favors the interpretation for the North Shillong Detachment to have developed in the Cretaceous during the separation of India from Antarctica (e.g., Powell et al., 1988; Srivastava et al., 2005; Ghosh et al., 2005). The best evidence supporting Cretaceous activity on the North Shillong Detachment comes from the work of Biswas et al. (2007). They showed Cretaceous U-Th/He and fission-track apatite cooling ages from samples located in the footwall of our mapped North Shillong Detachment. The thermal history of the northern Shillong Plateau as detected by modeling track-length distributions indicates rapid cooling between 95 Ma and 70 Ma (Biswas et al., 2007), which probably reflects the duration of motion on the North Shillong Detachment. We note that the lack of Cretaceous strata in the footwall of the ductile shear zone in the northern Shillong Plateau is also consistent with our interpretation that the North Shillong Detachment is a south-dipping Cretaceous structure (Fig. 2). This interpretation implies that the Cretaceous strata were absent in the footwall of the detachment fault in the northern Shillong Plateau at the onset of the India-Asia collision. This is consistent with the lack of Cretaceous strata in the eastern Himalaya (Bhargava, 1995; Kumar, 1997).

Cenozoic Deformation

Morphologically, the northern margin of the Shillong Plateau is not as sharply defined as the linear southern margin, and basement rocks are scattered across the Brahmaputra River Valley toward the Himalayan Range (Figs. 2 and 3). The northern margin of the plateau also makes several sharp left-step bends along which the Brahmaputra River course deflects (Figs. 2 and 3). Some of the deflections coincide with northeast-striking active left-slip faults (Fig. 3; also see following discussion).

Past investigators have focused mostly on the plateau-bounding structures and have treated the plateau as a rigid block (e.g., Bilham and England, 2001). Our work suggests that the plateau itself has also experienced extensive and detectable Cenozoic deformation, mostly expressed as active northeast-striking left-slip faults. This finding is consistent with the earthquake fault-plane solutions obtained across the Shillong Plateau, which indicate dominantly left-slip faulting on northeast-trending planes and right-slip faulting on the northwest-trending planes (Kayal and Zhao, 1998; Kayal et al., 2006). It is also consistent with a recent GPS study that implies a slip rate of ~5 mm/yr across the Badapani-Tyrsad shear zone (Jade et al., 2007). The northeast-striking left-slip faults may root all the way into the mantle, as suggested by the northeast-trending fastest direction of shear-wave polarization below the Shillong Plateau (Singh et al., 2006) and seismicity within the whole crust and upper mantle (Mitra et al., 2005).

The active left-slip faults are parallel to the dominant shear zones, thrusts, fold axes, and gneissic foliation in the Shillong basement and the Proterozoic Shillong Group, suggesting that their occurrence may have been controlled by preexisting fabrics. The high-angle relationship between the dominantly northeast-trending preexisting fabrics and the east-trending Cenozoic Shillong uplift in the Indian craton indicates that the development of the Shillong Plateau was not controlled by reactivation of preexisting weakness in the Indian craton during the India-Asian collision. The presence of the Cenozoic left-slip faults may also explain consistent apparent left-lateral offsets of the Brahmaputra River and the northern edge of the Shillong Plateau (Fig. 2B), which imply that the magnitude of left-slip motion on individual faults may range from 10 to 30 km.

Bilham and England (2001) emphasized the role of the south-dipping Oldham fault and suggested that its coeval motion with the north-dipping Dauki thrust to the south created the Shillong Plateau. As the Oldham fault is only present along the western half of the northern plateau margin, its motion cannot explain the uplift of the eastern Shillong Plateau or the Mikir Hills farther to the east. The extensive exposure of the basement rocks across the

Brahmaputra River Valley also requires the presence of an underlying north-dipping structure that could have uplifted both the Brahmaputra River Valley and the generally northward-tilting Shillong Plateau.

From the geodetic study of Bilham and England (2001), the Dauki thrust cannot be a simple low-angle planar structure dipping at ~30° because it would intersect the active high-angle Oldham fault in the north. We note that the Moho has an abrupt step immediately north and south of Cheerapunjee from ~44 km to ~38 km based on a receiver function study, possibly resulting from fault offset (Mitra et al., 2005) (Fig. 2B). We also note that the Moho is at a depth of ~39 km at a distance of ~60 km north of the Dauki thrust and lies at ~35 km below the central Shillong Plateau (Mitra et al., 2005) (Fig. 2B). The Moho depth increases gradually north of the Shillong Plateau, varying from 40 to 42 km across the Brahmaputra River valley to ~48 km immediately below the Main Central thrust in the eastern Himalaya. This regional dip of the Moho may be explained by a north-dipping thrust zone that cuts across the whole crust and locally duplicates the mantle lithosphere. In light of this model, the Brahmaputra River Valley is a composite basin. It is the foreland basin of the eastern Himalayan thrust belt and the piggyback basin of the lithospheric-scale Dauki thrust zone. The Oldham fault, despite having the ability to generate great earthquakes, is a back thrust of the overall south-directed thrust system in our interpretation (Fig. 2B).

Tectonic History of the Northeastern Indian Craton

From this discussion, we propose the following history for the tectonic development of northeastern India. Prior to deposition of the Shillong Group, the northeastern Indian craton experienced two episodes of magmatism at 1750–1600 Ma and 1150–950 Ma, as detected both by our direct dating of orthogneiss and the age clusters of detrital zircons from the Shillong Group. The magmatic events may have been related to arc development and subsequent continental collisions that built the proto-Indian continent (Figs. 11A and 11B). Specifically, the 1100 Ma event in northeastern India correlates well with the development of the Eastern Ghats orogenic belt during collision between India and Antarctica (e.g., Kelly et al., 2002) (Fig. 12). In addition to northernmost India, which is currently subducted below the Tibetan Plateau, India was probably linked with the Lhasa terrane at the time (e.g., Chang and Zheng, 1973; Allègre et al., 1984; Hsü et al., 1995; cf. Şengör, 1984). We suggest that

the first separation of India from Antarctica did not occur until the late Proterozoic during the deposition of the Shillong Group (Figs. 11C and 12). The presence of abundant quartz arenite and the lack of 520–480 Ma zircon ages support our interpretation that the Shillong Group was deposited in a passive-margin setting.

Less than 30 m.y. after the cessation of deposition of the Shillong Group, westward oceanic subduction (in present-day orientation) started below the eastern Indian margin and produced arc magmatism between 520 and 480 Ma (Figs. 11D and 12). The closure of the ocean between India and Antarctica led to the formation of Eastern Gondwana (e.g., Meert, 2003; Collins and Pisarevsky, 2005; Collins et al., 2007). Intense regional contraction occurred between 520 Ma and 500 Ma, which was expressed by the development of the Central Shillong thrust and isoclinal folding in the Shillong Group. Postkinematic plutons with ages ranging from 500 Ma to 480 Ma or even younger (i.e., undeformed granitoids in Fig. 3A) may have been generated after the collision between Antarctica and India (Fig. 11E).

Between 460 Ma and 140 Ma, northeastern India was part of stable Eastern Gondwana and received cratonal sediments mostly during the Permian (Fig. 11F). The cause of Permian sedimentation could have been due to a thermal event in the mantle or a change in sea level. The Mesozoic breakup of Eastern Gondwana was expressed by separation of the Lhasa terrane from India in the Late Triassic and Early Jurassic (e.g., Allègre et al., 1984; Yin and Harrison, 2000; Dai et al., 2008) and separation of Antarctica from India in the Cretaceous (e.g., Ghosh et al., 2005; Srivastava et al., 2005) (Fig. 12). The latter generated east-dipping extensional shear zones, as exemplified by the North Shillong Detachment (Fig. 11G). Cretaceous rifting was associated with synrift sedimentation and coeval intrusion and eruption of mafic rocks. Postrift sedimentation continued in the Late Cretaceous until the onset of contractional deformation at or prior to the middle Miocene (ca. 10 Ma) in the area (Figs. 11G and 11H) (Biswas et al., 2007). The uplift of the Shillong Plateau may have started in the early Miocene at ca. 23–20 Ma, as indicated by the progressive thinning of the Miocene strata from the Sylhet Trough to the plateau (Fig. 11I) (Evans, 1964). The development of the east-trending thrusts and folds along the southern edge of the Shillong Plateau was accompanied or immediately followed by the development of northeast-striking left-slip faults that remain active today (Fig. 2A).

Our model explains the contrasting lithology between the Lesser Himalayan Sequence

and the Greater Himalayan Crystalline Complex in the Cenozoic Himalayan orogen. The former lacks 500 Ma granites, whereas the latter has them. This contrast may be explained by our model such that the Greater Himalayan Crystalline Complex was located within the Cambrian-Ordovician arc, while the Lesser Himalayan Sequence was deposited in a retroarc setting. The two features may have been separated by a cratonward-directed early Proterozoic thrust belt as proposed Gehrels et al. (2003) (Fig. 12C).

CONCLUSIONS

Our combined structural and geochronological work reveals three episodes of igneous activity at ca. 1600 Ma, ca. 1100 Ma, and ca. 500 Ma, respectively. We relate the 1600 Ma event to the collision of two proto-India continental blocks, the 1100 Ma event to collision between India-Antarctica and Australia–South Tibet during the formation of Rodinia, and the 500 Ma event to the amalgamation of Eastern Gondwana. Our study also documents three ductile-deformation events at ca. 1100 Ma, 520–500 Ma, and during the Cretaceous. The first two events were contractional, induced by assembly of Rodinia and Eastern Gondwana, while the last event was extensional, related to breakup of Gondwana. Because of its proximity, the 500 Ma contractional deformation in the Shillong region implies that any attempt to determine the magnitude of Cenozoic deformation in the Himalaya using Proterozoic strata as marker beds must first remove the effects of early Paleozoic deformation. The chronostratigraphy of the Shillong Plateau established by this study implies that the Greater Himalayan Crystalline Complex is a tectonic mixture of Indian crystalline basement and its Proterozoic-Cambrian cover sequence intruded by an early Paleozoic arc. Although the Shillong Plateau has been treated as a rigid block during Cenozoic deformation, our work demonstrates that its interior is dominated by distributed active left-slip faults, an observation consistent with the existing fault-plane solutions in the region and which has important implications for future management of earthquake hazards in northeast India.
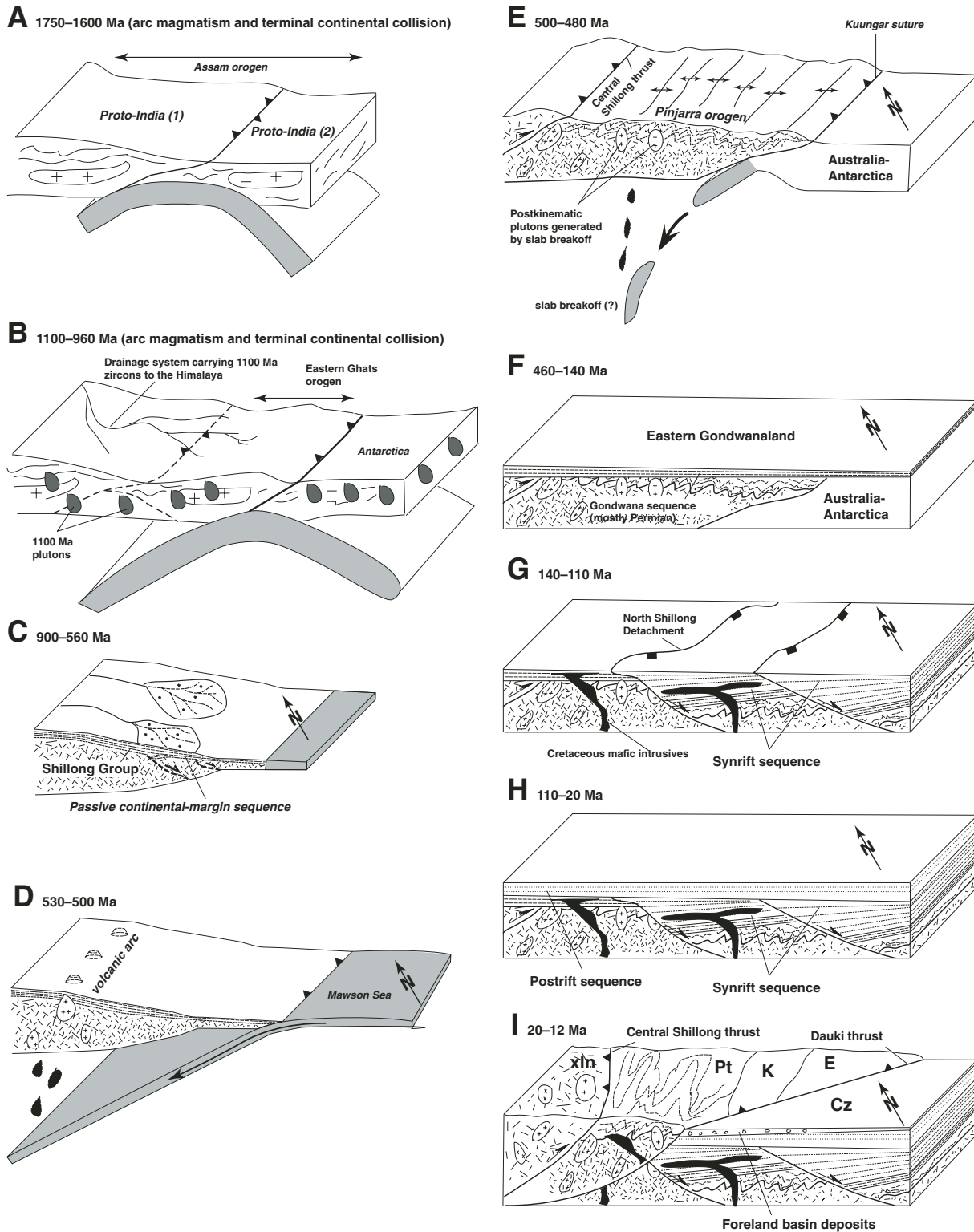
Figure 11. Schematic diagrams showing possible evolutionary history of northeastern India. (A) 1750–1600 Ma: magmatism and amalgamation of two proto-Indian continental blocks. (B) 1150–950 Ma: arc magmatism and collision of India-Antarctica and Australia along the Albany-Fraser belt. (C) 900 Ma(?)–560 Ma: deposition of the Shillong Group in a passive-margin setting. (D) 530–500 Ma: arc magmatism during subduction of the Mawson Sea. (E) 500–480 Ma: Contractional deformation related to final closure of the Mawson Sea and collision of India and Australia. Postkinematic plutons were emplaced into the highly deformed orogenic belt. (F) 460–140 Ma: stable Gondwana. (G) Breakup of Gondwana and the associated development of extensional faults and deposition of synrifting sediments. (H) 110–20 Ma: postrift sedimentation. (I) 20–12 Ma: initial uplift of the Cenozoic Shillong Plateau.
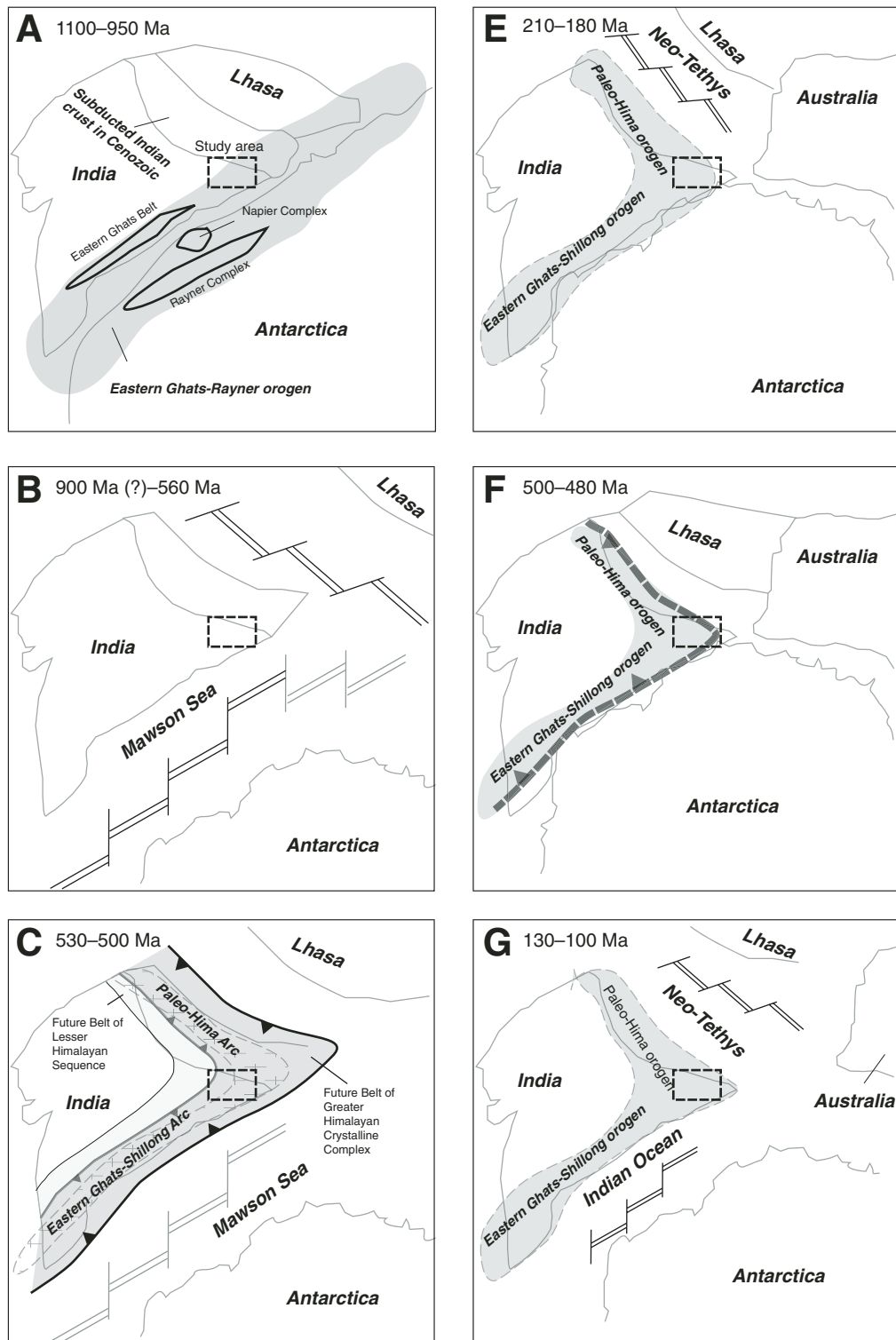
Figure 12. Tectonic evolution of northeastern India in the context of Gondwana evolution. (A) 1100–950 Ma: development of the Albany-Fraser orogen during ocean consumption and terminal collision between India-Antarctica and Australia-Tibetan terranes (Lhasa and Qiangtang). (B) 900 Ma(?)–560 Ma: separation of India from Antarctica and development of a passive continental margin along the east side of India. (C) 530–500 Ma: subduction of the Mawson Sea along the east and north sides of India and the development of the Eastern Ghats and paleo-Hima arcs. (D) 500–480 Ma: collision of India and Antarctica along the Eastern Ghats orogen and collision between India and Lhasa along the paleo-Hima orogen. (E) 210–180 Ma: separation of Lhasa terrane from India in Late Triassic and Early Jurassic and the birth of the Neotethys Ocean. (F) 130–100 Ma: separation of Antarctica from India and the birth of the Indian Ocean.

REFERENCES CITED

Allègre, C.J., and 34 others, 1984, Structure and evolution of the Himalayan-Tibet orogenic belt: Nature, v. 307, p. 17–22, doi: 10.1038/307017a0.

Ameen, S.M.M., Wilde, S.A., Kabir, Z., Akon, E., Chowdhury, K.R., and Khan, S.H., 2007, Paleoproterozoic granitoids in the basement of Bangladesh: A piece of the Indian shield or an exotic fragment of the Gondwana jigsaw?: Gondwana Research, v. 12, p. 380–387, doi: 10.1016/j.gr.2007.02.001.

Argles, T.W., Prince, C.I., Foster, G.L., and Vance, D., 1999, New garnets for old? Cautionary tales from young mountain belts: Earth and Planetary Science Letters, v. 172, p. 301–309, doi: 10.1016/S0012-821X(99)00209-5.

Azmi, R.J., and Paul, S.K., 2004, Discovery of Precambrian-Cambrian boundary protoconodonts from the Gangolihat Dolomite of Inner Kumaun Lesser Himalaya: Implication on age and correlation: Current Science, v. 86, p. 1653–1660.

Beaumont, C., Jamieson, R.A., Nguyen, M.H., and Lee, B., 2001, Himalayan tectonics explained by extrusion of a low-viscosity crustal channel coupled to focused surface denudation: Nature, v. 414, p. 738–742, doi: 10.1038/414738a.

Beaumont, C., Jamieson, R.A., Nguyen, M.H., and Medvedev, S., 2004, Crustal channel flows: 1. Numerical models with applications to the tectonics of the Himalayan-Tibetan orogen: Journal of Geophysical Research, v. 109, p. B06406, doi: 10.1029/2003JB002809.

Beaumont, C., Nguyen, M.H., Jamieson, R.A., and Ellis, S., 2006, Crustal flow models in large hot orogens, *in* Law, R.D., Searle, M.P., and Godin, L. eds., Channel Flow, Ductile Extrusion and Exhumation in Continental Collision Zones: Geological Society of London Special Publication 268, p. 91–145.

Bhargava, O.N., 1995, The Bhutan Himalaya: A Geological Account: Geological Survey of India Special Publication 39, 244 p.

Bilham, R., and England, P., 2001, Plateau 'pop-up' in the great 1897 Assam earthquake: Nature, v. 410, p. 806–809, doi: 10.1038/35071057.

Biswal, T.K., De Waele, B., and Ahuja, H., 2007, Timing and dynamics of the juxtaposition of the Eastern Ghats mobile belt against the Bhandara craton, India: A structural and zircon U-Pb SHRIMP study of the fold-thrust belt and associated nepheline syenite plutons: Tectonics, v. 26, p. TC4006, doi: 10.1029/2006TC002005.

Biswas, S., and Grasemann, B., 2005, Quantitative morphotectonics of the southern Shillong Plateau (Bangladesh/India): Australian Journal of Earth Sciences, v. 97, p. 82–03.

Biswas, S., Coutand, I., Grujic, D., Hager, C., Grasemann, B., and Stockli, D., 2006, Exhumation of the Shillong Plateau and its influence on Himalayan tectonics: Eos (Transactions, American Geophysical Union), fall meeting supplement, v. 88, abstract T13E–06.

Biswas, S., Coutand, I., Grujic, D., Hager, C., Stockli, D., and Grasemann, B., 2007, Exhumation and uplift of the Shillong Plateau and its influence on the eastern Himalayas: New constraints from apatite and zircon (U-Th-[Sm])/He and apatite fission track analyses: Tectonics, v. 26, p. TC6013, doi: 10.1029/2007TC002125.

Boger, S.D., Carson, C.J., Wilson, C.J.L., and Fanning, C.M., 2000, Neoproterozoic deformation in Radok Lake region of the northern Prince Charles Mountains, East Antarctica; evidence for a single protracted orogenic event: Precambrian Research, v. 104, p. 1–24, doi: 10.1016/S0301-9268(00)00079-6.

Catlos, E.J., Harrison, T.M., Manning, C.E., Grove, M., Rai, S.M., Hubbard, M.S., and Upreti, B.N., 2002, Records of the evolution of the Himalayan orogen from in situ Th-Pb ion microprobe dating of monazite: Eastern Nepal and western Garhwal: Journal of Asian Earth Sciences, v. 20, p. 459–479, doi: 10.1016/S1367-9120(01)00039-6.

Chang, C.-F., and Zheng, S.-L., 1973, Tectonic features of the Mount Jolmo Lungma region in southern Tibet, China: Scientia Geologica Sinica, v. 1, p. 1–12.

Chatterjee, N., Mazumdar, A.C., Bhattacharya, A., and Saikia, R.R., 2007, Mesoproterozoic granulites of the Shillong-Meghalaya Plateau: Evidence of westward continuation of the Prydz Bay Pan-African suture into northeastern India: Precambrian Research, v. 152, p. 1–26, doi: 10.1016/j.precamres.2006.08.011.

Clark, M.K., 2006, Late Miocene dismemberment of the Himalayan arc: Deformation of the Shillong Plateau, NE India: Eos (Transactions, American Geophysical Union), fall meeting supplement, v. 88, abstract T43E–02.

Coffin, M.F., Pringle, M.S., Duncan, R.A., Gladezenko, T.P., Storey, M., Muller, R.D., and Gahagan, L.A., 2002, Kerguelen hotspot magma output since 130 Ma: Journal of Petrology, v. 43, p. 1121–1139, doi: 10.1093/petrology/43.7.1121.

Collins, A.S., and Pisarevsky, S.A., 2005, Amalgamating eastern Gondwana: The evolution of the circum-Indian orogens: Earth-Science Reviews, v. 71, p. 229–270, doi: 10.1016/j.earscirev.2005.02.004.

Collins, A.S., Santosh, M., Braun, I., and Clark, C., 2007, Age and sedimentary provenance of the southern granulites, South India: U-Th-Pb SHRIMP secondary ion mass spectrometry: Precambrian Research, v. 155, p. 125–138, doi: 10.1016/j.precamres.2007.01.006.

Crawford, A.R., 1969, India, Ceylon and Pakistan: New age data and comparison with Australia: Nature, v. 223, p. 380–384, doi: 10.1038/223380a0.

Dai, J.G., Yin, A., Liu, W.C., and Wang, C.S., 2008, Nd isotopic compositions of the Tethyan Himalayan Sequence in southeastern Tibet: Science in China–Earth Science, v. 51D, p. 1306–1316.

Dalziel, I.W.D., 1991, Pacific margins of Laurentia and East Antarctica–Australia as a conjugate rift pair: Evidence and implications for an Eocambrian supercontinent: Geology, v. 19, p. 598–601, doi: 10.1130/0091-7613 (1991)019<0598:PMOLAE>2.3.CO;2.

Das Gupta, A.B., and Biswas, A.K., 2000, Geology of Assam: Banglore, Geological Society of India, 169 p.

DeCelles, P.G., Gehrels, G.E., Quade, J., LaReau, B., and Spurlin, M., 2000, Tectonic implications of U-Pb zircon ages of the Himalayan orogenic belt in Nepal: Science, v. 288, p. 497–499, doi: 10.1126/science.288.5465.497.

DiPietro, J.A., and Pogue, K.R., 2004, Tectonostratigraphic subdivisions of the Himalaya: A view from the west: Tectonics, v. 23, doi: 10.1029/2003TC001554.

Drukpa, D., Velasco, A.A., and Doser, D.I., 2006, Seismicity in the Kingdom of Bhutan (1937–2003): Evidence for crustal transcurrent deformation: Journal of Geophysical Research, v. 111, p. B06301, doi: 10.1029/2004JB003087.

Evans, P., 1964, The tectonic framework of Assam: Geological Society of India Journal, v. 5, p. 80–96.

Frank, W., Grasemann, B., Guntli, P., and Miller, C., 1995, Geological map of the Kishwar-Chamba-Kulu region (NW Himalayas, India): Jahrbuch der Geologischen Bundesanstalt, v. 138, p. 299–308.

Gansser, A., 1964, The Geology of the Himalayas: New York, Wiley Interscience, 289 p.

Gansser, A., 1983, Geology of the Bhutan Himalaya: Boston, Birkhäuser Verlag, 181 p.

Gehrels, G.E., DeCelles, P.G., Martin, A., Ojha, T.P., Pinhassi, G., and Upreti, B.N., 2003, Initiation of the Himalayan orogen as an early Paleozoic thin-skinned thrust belt: GSA Today, v. 13, no. 9, p. 4–9, doi: 10.1130/1052-5173(2003)13<4:IOTHOA>2.0.CO;2.

Gehrels, G.E., DeCelles, P.G., Ojha, T.P., and Upreti, B.N., 2006a, Geologic and U-Th-Pb geochronologic evidence for early Paleozoic tectonism in the Kathmandu thrust sheet, central Nepal Himalaya: Geological Society of America Bulletin, v. 118, p. 185–198, doi: 10.1130/B25753.1.

Gehrels, G.E, DeCelles, P.G., Ojha, T.P., Upreti, B.N., 2006b, Geologic and U-Pb geochronologic evidence for early Paleozoic tectonism in the Dadeldhura thrust sheet, far-west Nepal Himalaya: Journal of Asian Earth Sciences, v. 28, p. 385–408.

Ghosh, J.G., de Wit, M.J., and Zartman, R.E., 2004, Age and tectonic evolution of Neoproterozoic ductile shear zones in the southern granulite terrain of India, with implications for Gondwana studies: Tectonics, v. 23, p. TC3006, doi: 10.1029/2002TC001444.

Ghosh, S., Charkraborty, S., Bhalla, J.K., Paul, D.K., Sarkar, A., Bishui, P.K., and Gupta, S.N., 1991, Geochronol-ogy and geochemistry of granite plutons from east Khasi Hills, Meghalaya: Journal of the Geological Society of India, v. 37, p. 331–342.

Ghosh, S., Charkaborty, S., Paul, D.K., Bhalla, J.K., Bishui, P.K., and Gupta, S.N., 1994, New Rb-Sr isotopic ages and geochemistry of granitoids from Meghalaya and their significance in middle and late Proterozoic crustal evolution: Indian Minerals, v. 48, p. 33–44.

Ghosh, S., Fallick, A.E., Paul, D.K., and Potts, P.J., 2005, Geochemistry and origin of Neoproterozoic granitoids of Meghalaya, northeast India: Implications for linkage with amalgamation of Gondwana supercontinent: Gondwana Research, v. 8, p. 421–432, doi: 10.1016/S1342-937X(05)71144-8.

Grujic, D., Coutand, I., Bookhagen, B., Bonnet, S., Blythe, A., and Duncan, C., 2006, Climatic forcing of erosion, landscape, and tectonics in the Bhutan Himalayas: Geology, v. 34, p. 801–804, doi: 10.1130/G22648.1.

Gupta, R.P., and Sen, A.K., 1988, Imprints of Ninety-East Ridge in the Shillong Plateau, Indian Shield: Tectonophysics, v. 154, p. 335–341, doi: 10.1016/0040-1951(88)90111-4.

Heim, A., and Gansser, A., 1939, Central Himalaya Geological Observations of Swiss Expedition: Zurich, Société Helvétique des Sciences Naturelles, 246 p.

Hoffman, P.F., 1991, Did the breakout of Laurentia turn Gondwanaland inside out?: Science, v. 252, p. 1409–1412, doi: 10.1126/science.252.5011.1409.

Hsü, K., et al., 1995, Tectonic evolution of the Tibetan Plateau: A working hypothesis based on the archipelago model of orogenesis: International Geology Review, v. 37, p. 473–508.

Hughes, N.C., Peng, S.C., Bhargava, O.N., Ahluwalia, A.D., Walia, S., Myrow, P.M., and Parcha, S.K., 2005, Cambrian biostratigraphy of the Tal Group, Lesser Himalaya, India, and early Tsanglangpuan (late early Cambrian) trilobites from the Nigali Dhar syncline: Geological Magazine, v. 142, p. 57–80, doi: 10.1017/S0016756804000366.

Jade, S., et al., 2007, Estimates of interseismic deformation in northeast India from GPS measurements: Earth and Planetary Science Letters, v. 263, p. 221–234, doi: 10.1016/j.epsl.2007.08.031.

Johnson, S.Y., and Alam, A.M.N., 1991, Sedimentation and tectonics of the Sylhet Trough, Bangladesh: Geological Society of America Bulletin, v. 103, p. 1513–1527, doi: 10.1130/0016-7606(1991)103<1513:SATOTS>2.3.CO;2.

Kayal, J.R., and De, R., 1991, Microseismicity and tectonics in northeast India: Bulletin of the Seismological Society of America, v. 81, p. 131–138.

Kayal, J.R., and Zhao, D.P., 1998, Three-dimensional seismic structure beneath Shillong Plateau and Assam Valley, northeast India: Bulletin of the Seismological Society of America, v. 88, p. 667–676.

Kayal, J.R., Arefiev, S.S., Barua, S., Hazarika, D., Gogoi, N., Kumar, A., Chowdhury, S.N., and Kalita, S., 2006, Shillong Plateau earthquake in northeast India region: Complex tectonic model: Current Science, v. 91, p. 109–114.

Kelly, N.M., Clarke, G.L., and Fanning, C.M., 2002, A two-stage evolution of the Neoproterozoic Rayner structural episode: New U-Pb sensitive high-resolution ion microprobe constraints from the Oygarden Group, Kemp Land, East Antarctica: Precambrian Research, v. 116, p. 307–330, doi: 10.1016/S0301-9268(02)00028-1.

Kohn, M.J., Wieland, M.S., Parkinson, C.D., and Upreti, B.N., 2004, Miocene faulting at plate tectonic velocity in the Himalayan of central Nepal: Earth and Planetary Science Letters, v. 228, p. 299–310, doi: 10.1016/j.epsl.2004.10.007.

Kohn, M.J., Wieland, M.S., Parkinson, C.D., and Upreti, B.N., 2005, Five generations of monazite in Langtang gneisses: Implications for chronology of the Himalayan metamorphic core: Journal of Metamorphic Geology, v. 23, p. 399–406, doi: 10.1111/j.1525-1314.2005.00584.x.

Kumar, D., Mamallan, R., and Dwivedy, K.K., 1996, Carbonatite magmatism in northeast India: Journal of Southeast Asian Earth Sciences, v. 13, p. 145–158, doi: 10.1016/0743-9547(96)00016-5.

Kumar, G., 1997, Geology of Arunachal Pradesh: Banglore, Geological Society of India, 217 p.

Kumar, M.R., Raju, P.S., Devi, E.U., Saul, J., and Ramesh, D.S., 2004, Crustal structure variations in northeast India from converted phases: Geophysical Research Letters, v. 31, p. L17605, doi: 10.1029/2004GL020576.

Lacassin, R., Replumaz, A., and Leloup, P.H., 1998, Hairpin river loops and slip-sense inversion on Southeast Asian strike-slip faults: Geology, v. 26, p. 703–706, doi: 10.1130/0091-7613(1998)026<0703:HRLASS>2.3.CO;2.

Lal, R.K., Ackerrnand, D., Seifert, E., and Halder, S.K., 1978, Chemographic relationships in sapphirine-bearing rocks from Sonapahar, Assam, India: Contributions to Mineralogy and Petrology, v. 67, p. 169–187, doi: 10.1007/BF01046574.

LeFort, P., 1975, Himalayas—collided range—present knowledge of continental arc: American Journal of Science, v. A275, p. 1–44.

LeFort, P., 1996, Evolution of the Himalaya, *in* Yin, A., and Harrison, T.M., eds., The Tectonics of Asia: New York, Cambridge University Press, p. 95–106.

Li, Z.X., Bogdanova, S.V., Collins, A.S., Davidson, A., De Waele, B., Ernst, R.E., Fitzsimons, I.C.W., Fuck, R.A., Gladkochub, D.P., Jacobs, J., Karlstrom, K.E., Lu, S., Natapov, L.M., Pease, V., Pisarevsky, S.A., Thrane, K., and Vernikovsky, V., 2008, Assembly, configuration, and break-up history of Rodinia: A synthesis: Precambrian Geology, v. 160, p. 179–210, doi: 10.1016/j.precamres.2007.04.021.

Martin, A.J., Gehrels, G.E., and DeCelles, P.G., 2007, The tectonic significance of (U-Th)/Pb ages of monazite inclusions in garnet from the Himalaya of central Nepal: Chemical Geology, v. 244, p. 1–24, doi: 10.1016/j.chemgeo.2007.05.003.

McQuarrie, N., Robinson, D., Long, S., Tobagay, T., Grujic, D., Gehrels, G., and Ducea, M., 2008, Preliminary stratigraphic and structural architecture of Bhutan: Implications for along-strike architecture of the Himalayan system: Earth and Planetary Science Letters, v. 272, p. 105–117, doi: 10.1016/j.epsl.2008.04.030.

Meert, J.G., 2003, A synopsis of events related to the assembly of eastern Gondwana: Tectonophysics, v. 362, p. 1–40, doi: 10.1016/S0040-1951(02)00629-7.

Mezger, K., and Cosca, M.A., 1999, The thermal history of the Eastern Ghats Belt (India) as revealed by U-Pb and $^{40}Ar/^{39}Ar$ dating of metamorphic and magmatic minerals: Implications SWEAT correlation: Precambrian Research, v. 94, p. 251–271, doi: 10.1016/S0301-9268 (98)00118-1.

Miller, C., Klotzli, U., Frank, W., Thoni, M., and Grasemann, B., 2000, Proterozoic crustal evolution in the NW Himalaya (India) as recorded by circa 1.80 Ga mafic and 1.84 Ga granitic magmatism: Precambrian Research, v. 103, p. 191–206, doi: 10.1016/S0301-9268(00)00091-7.

Mitra, S.K., and Mitra, S.C., 2001, Tectonic setting of the Precambrian of the north-eastern India (Meghalaya Plateau) and age of the Shillong Group of rocks: Geological Survey of India Special Publication 64, p. 653–658.

Mitra, S., Priestley, K., Bhattqacharyya, A.K., and Gaur, V.K., 2005, Crustal structure and earthquake focal depths beneath northeastern India and southern Tibet: Geophysical Journal International, v. 160, p. 227–248, doi: 10.1111/j.1365-246X.2004.02470.x.

Moores, E.M., 1991, Southwest U.S.–East Antarctica (SWEAT) connection: A hypothesis: Geology, v. 19, p. 1–12, doi: 10.1130/0091-7613(1991)019<0425:SUSEAS>2.3.CO;2.

Murphy, M.A., 2007, Isotopic characteristics of the Gurla Mandhata metamorphic complex: Implications for the

architecture of the Himalayan orogen: Geology, v. 35, p. 983–986, doi: 10.1130/G23774A.1.

Myrow, P.M., Hughes, N.C., Paulsen, T.S., Williams, I.S., Parcha, S.D., Thompson, K.R., Bowering, S.A., Peng, S.C., and Ahluwalia, A.D., 2003, Integrated tectonostratigraphic analysis of the Himalaya and implications for its tectonic reconstruction: Earth and Planetary Science Letters, v. 212, p. 433–443, doi: 10.1016/S0012-821X(03)00280-2.

Nakata, T., 1989, Active faults of the Himalaya of India and Nepal, *in* Malinconica, L.L., Jr., and Lillie, R.L., eds., Tectonics of the Western Himalayas: Geological Society of America Special Paper 232, p. 243–264.

Nelson, K.D., et al., 1996, Partially molten middle crust beneath southern Tibet: Synthesis of Project INDEPTH results: Science, v. 274, p. 1684–1696, doi: 10.1126/science.274.5293.1684.

Paces, J.B., and Miller, J.D., 1993, Precise U-Pb age of the Duluth Complex and related mafic intrusions, northeastern Minnesota: Geochronological insights in physical, petrogenetic, paleomagnetic, and tectonomagmatic processes associated with the 1.1 Ga Midcontinent rift system: Journal of Geophysical Research, v. 98, p. 13,997–14,013, doi: 10.1029/93JB01159.

Pan, G.T., Ding, J., Yao, D., and Wang, L., 2004, Geological Map of Qinghai-Xiang (Tibet) Plateau and Adjacent Areas, Chengdu Institute of Geology and Mineral Resources, China Geological Survey: Chengdu, China, Chengdu Cartographic Publishing House, scale 1:1,500,000.

Powell, C.M., Roots, S.R., and Veevers, J.J., 1988, Prebreakup continental extension in East Gondwanaland and the early opening of the eastern Indian Ocean: Tectonophysics, v. 155, p. 261–283, doi: 10.1016/0040-1951(88)90269-7.

Quidelleur, X., Grove, M., Lovera, O.M., Harrison, T.M., Yin, A., and Ryerson, F.J., 1997, The thermal evolution and slip history of the Renbu Zedong thrust, southeastern Tibet: Journal of Geophysical Research, v. 102, p. 2659–2679.

Rajendran, C.P., Rajendran, K., Duarah, B.P., Baruah, S., and Earnest, A., 2004, Interpreting the style of faulting and paleoseismicity associated with the 1897 Shillong, northeast India, earthquake: Implications for regional tectonics: Tectonics, v. 23, doi: 10.1029/2003TC001605.

Ramesh D.S., Kumar M.R., Devi E.U., Raju P.S., Yuan X., 2005, Moho geometry and upper mantle images of northeast India: Geophysical Research Letters, v. 32, doi: 10.1029/2005GL022789.

Richards, A., Parrish, R., Harris, N., Argles, T., and Zhang, L., 2006, Correlation of lithotectonic units across the eastern Himalaya, Bhutan: Geology, v. 34, p. 341–344, doi: 10.1130/G22169.1.

Şengör, A.M.C., 1984, The Cimmeride orogenic system and the tectonics of Eurasia: Geological Society of America Special Paper 195, p. 1–82.

Shaw, R.K., Arima, M., Kagami, H., Fanning, C.M., Shiraishi, K., and Motoyoshi, Y., 1997, Proterozoic events in the Eastern Ghats granulite belt, India: Evidence from Rb-Sr, Sm-Nd systematics, and SHRIMP dating: The Journal of Geology, v. 105, p. 645–656.

Singh, A., Kumar, M.R., Raju, P.S., and Ramesh, D.S., 2006, Shear wave anisotropy of the northeast Indian lithosphere: Geophysical Research Letters, v. 33, p. L16302, doi: 10.1029/2006GL026106.

Srivastava, R.K., and Sinha, A.K., 2004a, Geochemistry of Early Cretaceous alkaline ultramafic-mafic complex

from Jasra, Karbi Anglong, and Shillong Plateau, northeastern India: Gondwana Research, v. 7, p. 549–561, doi: 10.1016/S1342-937X(05)70805-4.

Srivastava, R.K., and Sinha, A.K., 2004b, Early Cretaceous Sung Valley ultramafic-alkaline-carbonatite complex, Shillong Plateau, northeastern India: Petrological and genetic significance: Mineralogy and Petrology, v. 80, p. 241–263, doi: 10.1007/s00710-003-0025-1.

Srivastava, R.K., Heaman, L.A., Sinha, A.K., and Sun, S.H., 2005, Emplacement age and isotope geochemistry of Sung Valley alkaline-carbonatite complex, Shillong Plateau, northeastern India: Implications for primary carbonate melt and genesis of the associated silicate rocks: Lithos, v. 81, p. 33–54, doi: 10.1016/j.lithos.2004.09.017.

Stacey, J.S., and Kramers, J.D., 1975, Approximation of terrestrial lead isotope evolution by a two-stage model: Earth and Planetary Science Letters, v. 26, p. 207–221, doi: 10.1016/0012-821X(75)90088-6.

Steck, A., 2003, Geology of the NW Indian Himalaya: Eclogae Geologicae Helvetiae, v. 96, p. 147–213.

Tewari, V.C., 2001, Discovery and sedimentology of microstromatolites from Menga Limestone (Neoproterozoic/Vendian), Upper Subansiri district, Arunachal Pradesh, NE Himalaya, India: Current Science, v. 80, p. 1440–1444.

van Breemen, O., Bowes, D.R., Bhattacharyya, and Chowdhary, P.K., 1989, Late Proterozoic–early Paleozoic Rb-Sr whole and mineral ages for granite and pegmatite, Goalpara, Assam, India: Journal of the Geological Society of India, v. 33, p. 89–92.

Wiedenbeck, M., Hanchar, J.M., Peck, W.H., Sylvester, P., Valley, J., Whitehouse, M., Kronz, A., Morishita, Y., Nasdala, L., Fiebig, J., Franchi, I., Girard, J.P., Greenwood, R.C., Hinton, R., Kita, N., Mason, P.R.D., Norman, M., Ogasawara, M., Piccoli, P.M., Rhede, D., Satoh, H., Schulz-Dobrick, B., Skar, O., Spicuzza, M.J., Terada, K., Tindle, A., Togashi, S., Vennemann, T., Xie, Q., and Zheng, Y.F., 2004, Further characterisation of the 91500 zircon crystal: Geostandard and Geoanalysis Research, v. 28, p. 9–39, doi: 10.1111/j.1751-908X.2004.tb01041.x.

Yin, A., 2006, Cenozoic tectonic evolution of the Himalayan orogen as constrained by along-strike variation of structural geometry, exhumation history, and foreland sedimentation: Earth-Science Reviews, v. 76, p. 1–131, doi: 10.1016/j.earscirev.2005.05.004.

Yin, A., and Harrison, T.M., 2000, Geologic evolution of the Himalayan-Tibetan orogen: Annual Review of Earth and Planetary Sciences, v. 28, p. 211–280.

Yin, A., Dubey, C.S., Kelty, T.K., Gehrels, G.E., Chou, C.Y., Grove, M., and Lovera, O., 2006, Structural evolution of the Arunachal Himalaya and implications for asymmetric development of the Himalayan orogen: Current Science, v. 90, p. 195–206.

Yin, A., Dubey, C.S., Kelty, T.K., Webb, A.A.G., Harrison, T.M., Chou, C.Y., and Célérier, J., 2009, Geologic correlation of the Himalayan orogen and Indian craton (part 2): Structural geology, U-Pb zircon geochronology, and tectonic evolution of the south flank of the eastern Himalayan orogen: Geological Society of America Bulletin (in review).